2007

Manufacturing and characterization of high-aspect-ratio diffusive micro-mixers

Vamsidhar Palaparthy
Louisiana State University and Agricultural and Mechanical College, vpalap1@lsu.edu

MANUFACTURING AND CHARACTERIZATION OF HIGH-ASPECT- RATIO DIFFUSIVE MICRO-MIXERS

A Thesis

Submitted to the Graduate Faculty of the
Louisiana State University and
Agricultural and Mechanical College
in partial fulfillment of the
requirements for the degree of
Master of Science in Mechanical Engineering

in

The Department of Mechanical Engineering

by
Vamsidhar Palaparthy
B.S., Osmania University, India, 2003
May, 2007

To my parents
Lakshmi and Murthy Palaparthy
and brothers Ravi and Sai

Acknowledgements

I would like to thank my graduate advisor, Dr. Dimitris Nikitopoulos, for giving me an opportunity to work with him His support, encouragement and motivation through all these years made this project interesting. I would like to thank my committee members Dr. Michael Murphy and Dr. Steven Soper for their valuable suggestions. I would also like to thank Dr. Ramdevireddy, for accepting my request to be present in my committee.

I would like to extend my special thanks to Amit Maha for his patience and helping me at all times, whenever I needed. I would like to thank Taehyun Park, who helped me with the thermal bonding and also provided lively environment in the lab. Also would like to extend my gratitude and appreciation to my lab mate and friend Sudheer Rani, for his constant encouragement and positive attitude

I would also like to thank my roommates and friends Arvind, Raghu, Rupesh, Srinivas, Prasad, Diwakar, Sreedhar and Dinesh for making my stay enjoyable at LSU.

Finally I would like to thank my parents and brothers for their support and encouragement without them this would have never been possible.

Table of Contents

List of Tables

List of Figures

List of Symbols

ρ	Fluid density
ν	Kinematic viscosity
ΔP	Pressure difference, psi
μ	Dynamic viscosity, kg/m s
AR	Aspect Ratio
D_{12}	Binary mass diffusion coefficients, m^2/s
d_h	Hydraulic diameter, m
H	Channel depth, μm
L_m	Length of channel required for complete mixing, m
M	Molarity, mol/L
V	Volume of fluid, m^3
P	Fluid pressure, N/m^2
Q	Flow Rate, m^3/s
Re	Reynolds number
t	Time, s
w	channel width, m
t_M	mixture production time, s

Abstract

In the Ligase Detection Reaction (LDR) technique different chemical reagents of varying concentration are mixed with the by-products of the polymerase chain reaction (PCR) for the detection of low abundant cancer diagnostic markers [1]. An effective micro-mixer which is cheap, durable over a relatively broad range of flows with easy manufacturing is required in this process. This work is aimed at manufacturing mixers according to the required specifications with metrology at every manufacturing process to estimate the limits and tolerances during manufacturing and analyzing their efficiency both numerically and experimentally.

An optimum mixer design developed earlier by Maha *et.al* [2] is used for this study. Additional numerical simulations are performed using Fluent on this mixer design for varying flow ratios in mixing streams. Micro milled mold insert is used to fabricate micro-mixers using the hot embossing process. These hot-embossed polymer based mixers are used in a micro-fluidic module that was designed and developed to carry out the LDR [1]. Micro channels with an aspect ratio of 12 are achieved which are further used for mixing experiments involving a Rhodamine B fluorescent dye solution and deionized water. An inverted epi-flourescent microscope setup with a continuous flow mercury lamp is used to observe the fluorescence signal.

Chapter 1. Introduction

Miniaturization of fluidic systems to carry out micro scale reactions and bio-analysis systems leading to “lab-on-chip” devices has been the wide area of research interest for the past many years. Some of the main applications being the Ligase Detection Reaction and Polymerase Chain Reaction which require chip mixing of reagents and delivery of mixed products. Many micro-mixer designs are available in literature; many have been developed and used. Based on the type of end use, the parameters that go into designing and subsequent manufacturing methodology of these micro-mixers varies. As categorized in literature these micro-mixers are of two types: Passive and active micro-mixers. Due to the arising need for low cost and biocompatibility, polymers are extensively used for these micro analysis systems, which lead to the development of different micro-fabrication techniques. Some of them being LIGA, (an acronym standing for the main steps of the process, ie., deep X-ray lithography, electroforming, and plastic molding), Laser Ablation, and Micro-milling.

Our current work has been focused on batch production of diffusional (passive) micro-mixers using micro-milled mold insert and subsequent hot-embossing to produce high aspect ratio micro channels. Metrology is done at each step in the production of micro-mixers to estimate the tolerance values which would give us an estimate of the exact dimensions to be used at the design level of these micro-channels. An aspect ratio of 6 is easily achievable using micro-milling and hot embossing processes for our current mixer designs.

In thebatch delivery of mixed product at the outlet of the mixer, the important parameter to be discussed is the mixture production time which itself is not only the

diffusion time for the two fluids (involved in a binary mixer) to mix, but also includes the time taken to deliver the required volume of mixed product up to the outlet of the mixer plus the time spent for the mixed reagents to come in contact with each other. Efforts are being made to reduce this mixture production time by controlling the flow ratio of the reagents in a high aspect ratio micro channel.

Jets in cross flow micro-mixers are manufactured using micro-milled mold insert and hot embossing process. Three of these mixers are laid on a single mold-insert two of which have same dimensions and the third mixer has double the dimensions. Addition of similar mixers increases additional mixers to test with minimal embossing effort. Embossed channels with an aspect ratio of twelve were manufactured.. To obtain minimum mixture production time and achieve efficient mixing of fluids in a three stream fluid layer, simulations with different flow ratios were performed and the mixing efficiencies were evaluated based on various definitions. Results from the experiments are compared with the numerical results.

A review of various micro-mixers and their manufacturing processes along with the theory behind an optimal batch production micro-mixer is provided in Chapter 2. The manufacturing methodology involved in the production of diffusion based passive micro-mixer and it's metrology aspects are detailed in Chapter 3. Numerical simulations results for different flow ratios and the experimental validation of these results form Chapter 4. Future work and conclusions are provided in Chapter 5.

Chapter 2. Background

2.1 Literature Review

Due to low Reynolds numbers arising due to small dimensions , the benefits of turbulent mixing cannot be seen in micro channels. Mixing in micro channels is dominated by diffusion as fluid flow is laminar. Many different micro-mixers have been developed corresponding to different applications and are currently in use. These mixers are classified into passive and active. Maha in his thesis (2005) describes about various active and passive mixer designs from literature. Some are listed here along with the fabrication processes involved with them.

2.1.1 Active Mixers

Active mixers utilize the effect of external forces on the fluid flow to enhance mixing in micro channels. These external forces can be electrical, magnetic, pressure variations, and thermal forces. Evans et al (1997) introduced one of the first pulsed flow micro mixer. It is the first of its kind to improve mixing by inducing flow pulses. The device is fabricated using five mask process and subsequent etching onto silicon substrate. Hiroaki et al (2002) developed a magnetic force based chaotic micro-mixer for mixing of magnetic beads in bio-fluids. The fabrication process involves several steps right from KOH etching for fluid flows and etching with Deep Reactive Ion Etching (DRIE). Channel is formed by SU-8 and PECVD oxide, deposited with bonded cover glass to close the channel. Lu et al (2002) fabricated a single magnetic bar or an array of them to rotate rapidly within a fluid environment creating a rotating magnetic field to enhance mixing. Oddy et al (2001) developed a electrokinetic process to rapidly stir

microflow streams by initiating flow instability by oscillating electroosmotic channel flows sinusoidally.

2.1.2 Passive Mixers

Unlike active mixers, these type of mixers do not require any external force for mixing. Additional fabrication problems go into the manufacturing of active mixers which are not present in the case of passive ones. It is a known fact that manufacturing of passive mixers is much simpler and easier due to the absence of moving or rotating parts as in the case of active ones. Stroock et al (2002) presented a passive mixer to mix fluid flows at low Reynolds numbers in micro channels using chaotic advection. They used bas-relief structures on the floor of the channel that are easily fabricated with commonly used methods of planar lithography. Maha et al (2003) simulated various diffusional based micro-mixer designs and proposed jets in cross flow performs best. Liu et al (2000) proposed a three-dimensional serpentine micro-channel design as a means of implementing chaotic advection to enhance passive mixing. Using double sided KOH wet-etching technique, the micro-mixer was fabricated in a silicon wafer. Chung et al designed a micro-mixer that was actuated by a pneumatic pump to induce self-circulation of the fluid in the mixing chamber. They constructed the device with two poly-methylmethacrylate (PMMA) layers, while upper layer was blank, structures of the component were built on lower PMMA layer using a CNC high-speed engraving and milling machine. After bonding the two PMMA layers and drilling two 1.5 mm diameter holes to form liquid inlets and outlets, a complete PMMA block 50 mm long, 50 mm wide and 15 mm high was fabricated.

2.2 Theory for Optimal Diffusion Based Micro-Mixer for Batch Production

The theory of mixing in micro-channels is well explained by Nikitopoulos, D.E and Maha A. in chapter 7 of Micromixers [1]. To have batch delivery of mixed product from a micro mixer, the corresponding mixture production time is not only the diffusion time but should also include the time taken for the reagents to come in contact with each other and the time required by the mixer to deliver the volume of mixed fluid.

Considering a two stream batch production micro scale mixer of channel width *w,* height *H* and length *L*, the estimates given in theory for mixture production time (t_M) and necessary mixer channel length, *L* are given by

$$t_M = \frac{1}{4}\phi^2 \frac{w^2}{D_{12}} + \frac{V}{Q}, \tag{1}$$

$$L = \frac{1}{4}\phi^2 \frac{Q}{AR\, D_{12}} \tag{2}$$

where $\phi = \frac{w_{s\max}}{w}$, the ratio of width of the widest internal stream layer or twice the width of the widest wall bounded layer whichever is largest and the width of the channel, is defined as the diffusion width fraction.

D_{12}, is the binary mass diffusion coefficient.

V is the volume of mixed product

Q is the total flow rate (sum of individual flow rates into the mixing channels, Q_1 and Q_2)

AR =H/w is the aspect ratio of the channels.

In the mixer described above with two streams entering a mixing channel, the initial widths of the streams in the mixing channel after they come to contact is determined by the stream flow rates before they make the contact. One reason for this is that for flows in micro-channels with low Reynolds numbers wherein viscosity dominates, the momentum discontinuities occurring due to individual streams entering into one another in a mixing channel are smoothed resulting in short entrance length. Thus for modest Reynolds number flows in micro channels, the entrance length is a fraction of hydraulic diameter. Another being higher order (10^3 to 10^5) Schmidt number, $Sc = \nu/D_{12,}$ which shows that mass diffusion is much lower than momentum diffusion.

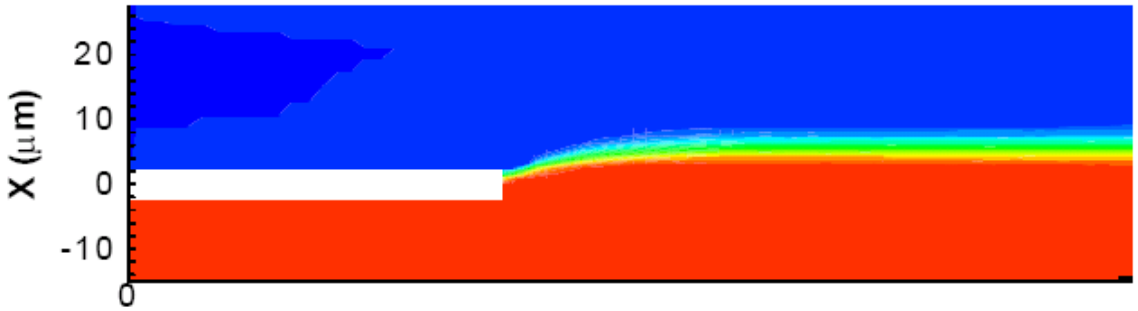

Figure 2.1 Two streams Blue and Red of widths 25μm and 12.5μm, in a mixing channel 42.5μm wide and 150μm high. D_{12}=1.2x10^{-10}m^2/s, Sc=8300 and Re=0.78[1]

Therefore, in a steady laminar flow with multiple streams entering a mixing channel, the flow becomes fully developed, even though the individual streams are still un-mixed. It is illustrated in the Figure 2.1 where two different streams with unequal widths and unequal average velocities, but with equal flow rates merge into a single mixing channel. It can be seen from the figure, that due to the symmetry of velocity profile for fully developed laminar flow in a rectangular ducts and also due to equal flow rates of merging streams, width of each fluid stream in the mixing channel after the development region is equal to one half of the mixing channel.

The value of ϕ can be estimated from the discussion above and for optimum performance a layered mixer is to be operated at specific flow rate ratios. In order to reduce the diffusion length due to layering of individual streams in the mixing channel, the minimum value of ϕ should be *1/(n-1)*, where *'n'* is the number of mixing streams. The ratio of volumetric flow rates can then be written as,

$$\psi_n = \frac{Q_1}{Q_2} \tag{3}$$

The optimum flow rate ratio ψ_o, with respect to the channel aspect ratio for multi-stream micro-mixers is shown in the Figure 2.2. For even number of feeding streams into the mixing channel, the value of ψ_o equals to 1. For a three layer mixer with aspect ratio of three and above this value corresponds to 2.2.

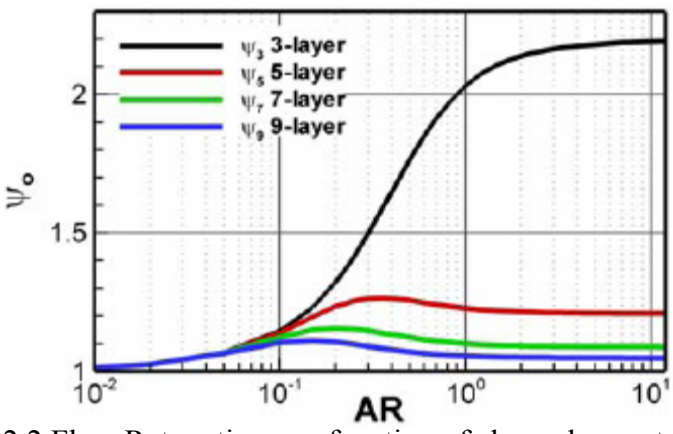

Figure 2.2 Flow Rate ratios as a function of channel aspect ratio [1].

For a given application, the theoretical optimum volumetric flow-rate values given in Table 2.1 are useful to design an optimum micro-channel mixer. Two different approaches for the design to be considered are:

Table 2.1 Stream-wise volumetric flow rates as a % of total mixture volumetric flow rate and their dependence on channel aspect ratio

Type	ψ_o	***AR***	Q_1(%)	Q_2(%)	Q_3(%)	Q_4(%)	Q_5(%)
3 streams	1.14	0.1	23.3	53.4	23.3	N/A	N/A
	1.41	0.25	20.7	58.5	20.7	N/A	N/A
	1.76	0.5	18.1	63.8	18.1	N/A	N/A
	2.03	1	16.5	67	16.5	N/A	N/A
	2.14	2	15.9	68.1	15.9	N/A	N/A
	2.18	4	15.7	68.5	15.7	N/A	N/A
	2.19	10	15.7	68.7	15.7	N/A	N/A
4 streams	1.00	0.1	14.4	35.6	35.6	14.4	N/A
	1.00	0.25	11.6	38.4	38.4	11.6	N/A
	1.00	0.5	9.3	40.7	40.7	9.3	N/A
	1.00	1	8.1	41.9	41.9	8.1	N/A
	1.00	2	7.6	42.4	42.4	7.6	N/A
	1.00	4	7.5	42.5	42.5	7.5	N/A
	1.00	10	7.4	42.6	42.6	7.4	N/A
5 streams	1.14	0.1	10	26.6	26.7	26.6	10
	1.25	0.25	7.4	27.8	29.5	27.8	7.4
	1.26	0.5	5.7	27.8	33	27.8	5.7
	1.23	1	4.8	27.5	35.4	27.5	4.8
	1.21	2	4.5	27.4	36.3	27.4	4.5
	1.21	4	4.4	27.4	36.5	27.4	4.4

1. a design that will produce the desired volume, V, at minimum production time for specified acceptable pressure loss in the device, or
2. a design that will produce the desired volume, V, at a minimum pressure loss for specified acceptable mixture production time.

$$Q = \frac{(-\Delta p)w^4}{12 L_M \mu} g(AR) \tag{4}$$

Equation 4 gives a relationship between pressure loss (-Δ*p*), total mixture flow rate Q. Combining this equation along with equations (1) and (2) will provide us simple basis to identify the appropriate design for a micro-mixer.

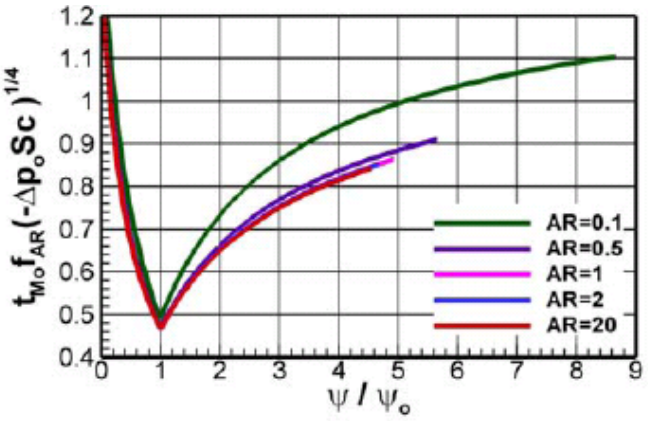

Figure 2.3 Scaled optimum mixture production time as a function of the flow rate ratio for a 3-stream micro-mixer[1]

Using figure 2.3, one can determine the minimum mixture production time in case of first approach or minimum pressure loss in case of second approach. Accordingly, after selecting the approach needed for a particular mixer design, length of mixing channel, L_o, is determined from Figure 2.4, mixture flow rate, Q_o, from Figure 2.5 and appropriate mixing channel width, w_o, from Figure 2.6

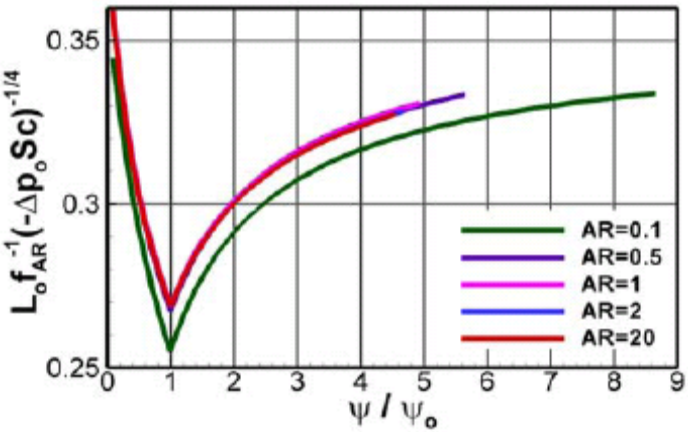

Figure 2.4 Scaled optimum mixing channel length as a function of flow rate ratio for a 3-stream micro-mixer[1]

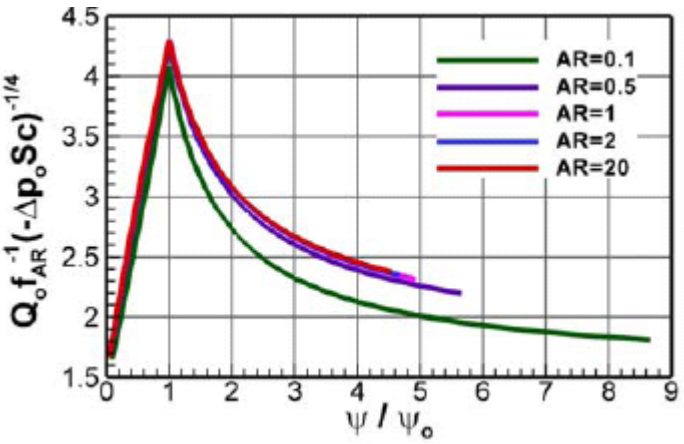

Figure 2.5 Scaled optimum volumetric flow rate as a function of flow rate ratio for 3-stream micro-mixer[1]

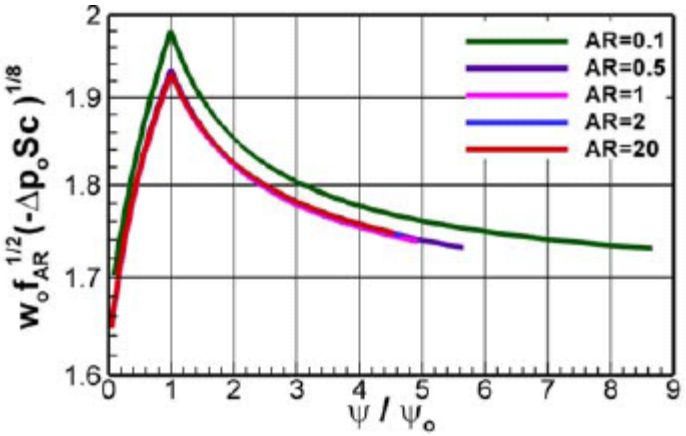

Figure 2.6 Scaled optimum mixing channel width as a function of flow rate ratio for 3-stream micro-mixer[1]

Having described the optimum parameters necessary for the design of a micro-mixer for a particular type of application and following one of the design criteria described above, one can choose different state of the art micro fabrication techniques to manufacture micro-channels.

Research and development in the field of Micro Electro Mechanical Systems (MEMS) led to various micro-fabrication methods which are widely in use today to produce high aspect ratio micro channels pertaining to a particular application. McAuley et al, using DRIE for channel widths of about 5μm were releasable in silicon, with aspect

ratios up to 50. New technologies like SU-8 Lithography, Laser Ablation, Micro-milling, Hot Embossing, and LIGA are being developed which involve manufacturing polymers like polymethylmethacrylate (PMMA) and Polycarbonate (PC) for micro analysis systems. Barret (2004) has done extensive work in these micro-fabrication methods and gives detailed information about each one in his thesis.

Micro-milling is one of the fabrication methods using which mold inserts are prepared that are used for mass production of polymer based micro channels using Hot-Embossing. This is one of the cheap and quickest methods in realizing the micro channels of considerable aspect ratios.

Chapter 3. Manufacturing and Characterization

3.1 Micro-Mixer Designs

As discussed in Chapter 2, of all the micro mixer designs in literature, the jets in cross flow type mixers designed and simulated by *Maha* (thesis 2005) perform better than any other designs. This particular design is mass produced using the fabrication methods available for quick and cost-effective output in production. Efforts have been made to produce mixers having high aspect ratio of about 12 using hot embossing process. Due to the inability, the aspect ratio was dropped to six. Three jets in cross flow type mixer designs are laid on the mold insert with first two of the same type and dimensions and the latter one having double the dimensions, thereby increasing the ability to test more mixers with less embossing effort.

3.2 Micro-Fabrication

There are many micro-fabrication techniques that are currently in use which are based on the technologies of microelectromechanical systems (MEMS). Some of the methods that are widely in use are listed below.

Laser Ablation,

SU-8 lithography,

LIGA,

Micro-milling.

The first two are direct methods of fabrication while the next two are indirect. Micro milling, a mass production technique, one of the indirect methods is chosen to fabricate micro-mixers for our study.

3.2.1 Micro Milling

A mold insert is prepared using a micro milling machine (Kern MMP – Microtechnic, Murnau-Westried, Germany) available at Center for Bio-Modular Microsystems, LSU. It consists of a stage which can be moved, a cutting tool holder, source of light and a computer using which the machine is controlled. A maximum spindle speed of about 40,000 rpm can be achieved, useful to produce clean cuts on the metal surface. The machine also consists of an infrared touch probe which automatically gives datum measurements of work piece, a laser measuring system for automatic determination of tool length and radius. A Panasonic CCD camera with Navitar Zoom 6000 microscope is also attached to the machine for real time observation of machining progress. Drawings of the features on the mold insert are given as an input to the computer connected to the micro-milling machine. Using GIBBS (Gibbs CAM 2004, Moorpark, CA) CAD/CAM software, these drawings are converted into CAM or machine language to transfer the features onto the metal surface. Debris due to machining is removed using compressed air.

The tool holder has a capability to hold 24 different tools. These tool bits are made of solid carbide. Selection of tool bits depends on the type of substrate used for the mold insert. Generally these tool bits have a cutting life of 20 hours which also depends on the substrate material. The least size of the tool bit that was used for machining had a tool bit tip roundness of 50μm. This had rounded corners on the mold insert instead of sharp 90-degree at intersections of two or more channels. Brass (353 brass alloy) is used as a substrate because of its good machining capability and low hardness which increases the tool life.

Figure 3.1 Kern MMP Micro-Milling Machine

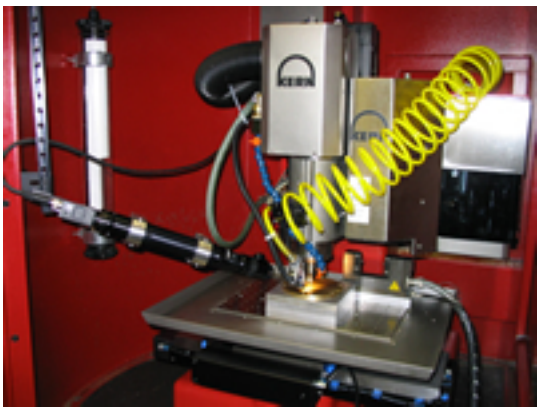

Figure 3.2 Closer view of Work stage. (Images courtesy : CBMM)

Also there is no use for a lubricant while machining brass and can also withstand embossing temperatures without any damage to the features. Thickness of the brass discs is about 5mm and about five inches in diameter. Counter sunk holes drilled around the disc are used to fix the mold insert onto the hot embossing machine plate to keep it in position while performing embossing. This mold insert combined with the hot-embossing process is typically used for mass production of the micro fluidic analysis systems.

3.2.2 Hot-Embossing

This is one of the most widely used mass production method to produce chips used for bio-medical analysis. The micro-milled mold insert with the features is hot-embossed onto polymethylmethacrylate (PMMA) a polymer based material. Before embossing, the mold insert is cleaned using di-water and soaked in iodine solution for a couple of hours to remove any dust particles and is again cleaned with de-ionized water. The embossing machine available here at LSU contains a lower plate onto which the

polymer is placed and kept in place by a ring which is then screwed on to the plate. The mold insert goes to the upper plate using counter sunk screws. The upper plate is preheated to 450 degrees before placing it onto the lower plate. Mold insert is fixed using screws which go into the counter sunk holes on the insert avoiding imprints of the screws on the chips. The hot upper plate with the mold insert fixed, is then carefully placed onto the lower plate while pulling vacuum in the lower plate. Care is taken so that the upper plate will not fall into the lower plate and the features partially get into the heated polymer chip while vacuum is pulled. This caused some air get trapped in before applying pressure for embossing which resulted in damages to the channels near rounded corners and channel widths of 12.5 microns. To fix this problem, stoppers are placed in between the top and bottom plates before they come to contact when vacuum is pulled.

The chips were hot-embossed at the LSU Center for Advanced Microstructures and Devices (CAMD), using a HEX 02 embossing machine (JENOPTIK Mikrotechnik, Jena, Germany). The temperature of the plate holding the mold insert is about 150 degrees centigrade. 20kN force applied for about 120 seconds and de-molding performed at 100 degrees centigrade are some of the other specs found by Datta *et.al* for hot-embossing using this machine. The mixers are embossed into polymethylmethacrylate (PMMA), a polymer based material.

After embossing these PMMA blanks with the mixers are covered with green tape to protect the channels from any foreign particles. These blanks are then cut using a band saw into small rectangular shape of 3 x 5 inches to account for easy mounting on to the microscope.

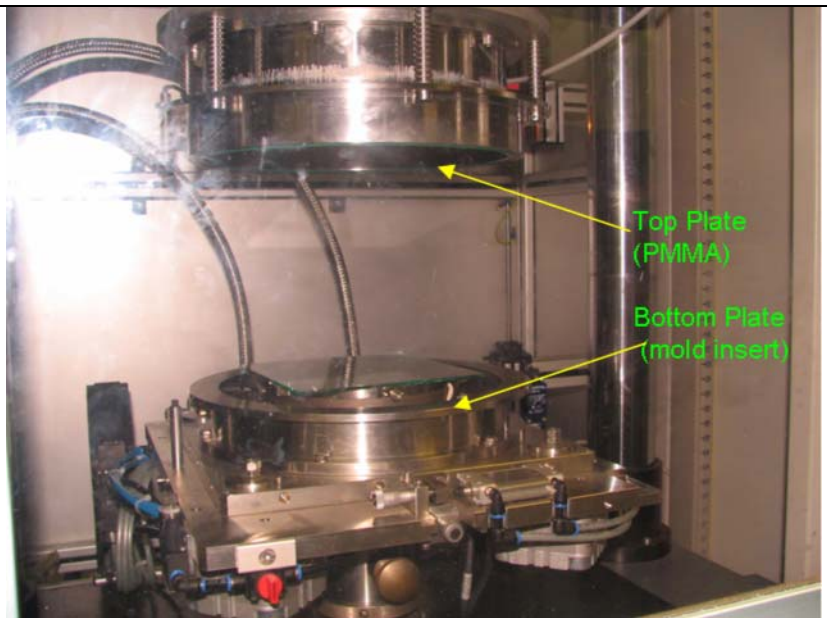

Figure 3.3 HEX 02 Hot Embossing Machine at CAMD

3.2.3 Drilling

Using micron hand drilling machine, holes of diameter 1mm are drilled into the reservoirs of these micro channels through which the fluid flows. Very low rpm is used while drilling holes into these reservoirs. At high speeds, the heat generated melts the polymer locally and solidifies creating burrs on or inside the channels which obstruct the fluid flow. Hence very low rpm of about 25-30 revolutions per min is used to drill holes using the 1mm drill bit. Also, coolant (drilling oil) is added while drilling so as to protect the drill bit life and to remove the heat generated due to friction. Holes are drilled from the channel reservoir through into the other side of the chip which gives us the capability to drill hole at the center of the reservoir unlike drilling from the other side, we are not sure if the hole ends in the reservoir or not. A slight deviation also would cause damage to the channel leading to leakage even after covering with the cover-slip. The machine has the capability to set the depth up to which we want the drill-bit to advance in order to

complete the hole through the channel. For each mixer three holes are drilled, one at each of the inlet reservoirs and one at the exit of the mixer.

3.2.4 Cleaning

The micro channels are to be cleaned without any dust particles which would make thermal bonding easy and successful. Presence of any dust particles would either not bond the cover perfectly well onto the chip or there would be some dust particles left out in the channels which will block the channels and obstruct fluid flow and removal of these particles would be impossible once the chip has been bonded.

The green tape is removed and the chip is cleaned first with di-water. It is then sonicated in a solution of di-water and IP8 solution, to remove any burrs and dust particles that might have stuck in the channels while cutting or drilling. Compressed air at high pressure is blown through the channels to remove any remaining particles sticking to the walls and to remove them. The channels are observed through microscope to check for presence of any dust particles which would otherwise block the flow in these channels. If any particles are present in the channels, cleaning is done before proceeding to the next step of covering the channels.

3.2.5 Thermal Bonding

The chips are to be covered with a cover slip for the fluid to flow through them. The cover sheet and chip are thermally bonded under uniform pressure to make sure that there is no leakage between them. Before bonding, the chip is to be cleaned well and checked for flatness to make bonding successful. The chips are warped due to induced strain while embossing and drilling and have to be straightened and made flat before bonding. The procedure followed is described in steps in the flow chart given. Cleaned

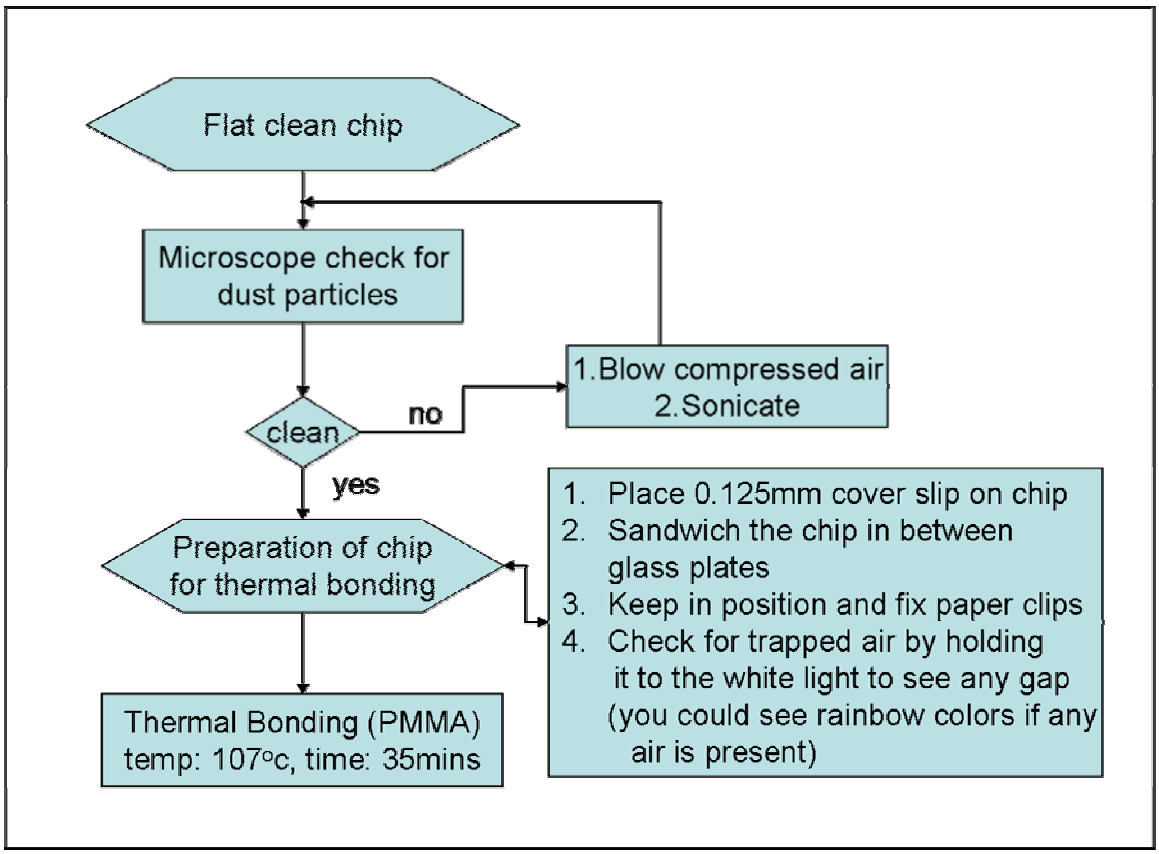

Figure 3.4 Flowchart for Thermal Bonding of PMMA chip

chip is covered with a 0.125mm cover sheer of PMMA and is sandwiched between two cleaned glass plates of thickness about 6mm and are clamped using paper clips. Chips are then checked for any trapped air in between the cover-slip and the chip by holding the sandwiched chip with the paper clips onto the white light. It is then kept in the preheated oven at 90 degrees centigrade. The temperature is increased to 107 degrees and is maintained at this temperature for about 35 minutes and allowed to cool in the oven once the bonding temperature and time are reached. This temperature and time used for bonding is a result of number of trials and is applicable only for PMMA samples, while for Polycarbonate (PC) chips the temperature as well as time required for bonding would be high. After the chip is bonded, it is tested for any leaks by physical examination.

Leak test is performed on the chip by blowing air through syringes. One can notice the bubbles coming out when the chip is placed in water while blowing air, only through the exit port which shows that bonding is good. Another test can also be done by pushing any colored dye (Rhodamine B) through the inlet channels and any leak in bonding can be noticed by the flow of the dye outside the channels.

Plastic tubing is fixed into the inlet reservoirs using Super Glue at the end of each tube. Another way of connecting tubes to the reservoirs is by using square shape connectors which have internal threads, and the tubing with externally threaded connectors is fixed into one another without leakage. Fluids are pushed into the channels using syringes which are driven by syringe pump.

3.3 Metrology and Characterization

Metrology is done on mold insert and also on embossed polymer chips to evaluate the tolerance values for the manufacturing processes in production of micro-mixers on large scale. This would help us determine the actual dimensions one should use at bench level drawing to achieve the final dimensions in the fabricated product that is used for the experiments. Measurements are taken at each and every critical location both on the mold insert and also on the embossed polymer chip to compare the changes in dimensions.

3.3.1 Stylus Profilometer

Profilometer is run on the mold insert at critical locations like the corners of the channels, junction of two or more channels, inlets to the mixing channels, reservoirs and exit channel widths to measure the height of the features milled on the mold insert and report the changes in height from one point to another. These critical locations are shown in the outline drawing of the mixer. Access to change the conditions set-forth on the

profilometer is restricted. Some of these conditions set-forth are, force used on the stylus indent is about 2mg, length of scan 1000μm, speed 50μm/sec in direction from left to right. The stylus runs on the particular location and records the measured data on a plot which gives the final averaged height of the features on the mold insert.

Table 3.1 Stylus Color codes, Radius and Shank Angles

Color Code Band	Stylus Radius(μm)	Shank Angle (Degrees)
Red	12.5	60
Yellow	5.0	60
Green	2.0	60
Black[a]	0.3-0.8	70
Black[a]	0.1-0.2	70

Due to the taper on the indent of the profilometer, it cannot be run at edges of the vertical walls. A flat surface on the bottom is taken as reference and feature height measured with reference to this bottom is reported. One can even measure the widths of the channels along with the feature height from the stylus profilometer reports, by actually calibrating the graphs and measuring the travel width of the stylus indent on the mold insert using some image processing software like Scion Image.

3.3.2 Scanning Electron Microscopy (SEM)

SEM was used to obtain two and three dimensional images of the mold insert features. The rationale for using this method is to measure the widths of the channels from the images obtained from SEM. The limit of resolution of SEM is approximately 4nm. The mold insert is placed on an aluminum disc which is then inserted into the SEM machine and electron beam is passed and images are taken. These images have a scale printed on them using which the actual length of the feature relative to the image can be measured using image processing software like Scion Image.

3.3.3 Image Processing

Images obtained from SEM are processed using Scion Image available for free from Scion Corporation. Images are loaded in .tiff format into the software to process them. These are calibrated based on the scale given on them and the measurements of the widths are taken based on these calibrations. Different images have different calibration values, but the method adopted is the same in all those cases. The software is capable of measuring widths, given the sharp edges within which we need the dimension. It can also measure the radius of the rounded corners on the channels. Only widths from the 2-dimensional images are measured.

3.3.4 Hot Embossed Chips

Embossed chips from the mold insert are cleaned and before they are thermally bonded, measurements are made on the chips using the indirect measurement using SEM and Scion Image software. The widths of the embossed channels on these chips are measured and are compared with those of the mold insert to get an estimate of the change in dimensions from mold insert to the embossed channel. This would lead us to the actual dimensions that should be used while designing the mixer. Using student-t distribution, the tolerance limits for different manufacturing procedures are evaluated based on the dimensions measured using different measuring methods.

3.3.5 Characteristic Distribution Methods

The course material is referred for this particular section. (ME7953: 2004-05)

3.3.5.1 Distribution of the Sample Mean When the Variance Is Known

For a given data sample consisting of measurements taken randomly at a particular location, the mean value of the sample is given as

$$\overline{X} = \frac{1}{N}\sum_{i=1}^{N} X_i \tag{5}$$

for N>10 the distribution of $\overline{X}$ approaches a normal distribution regardless of the distribution of X.

$$\text{Probability}\left[\overline{X} > \left(\frac{\sigma_X \eta_\alpha}{\sqrt{N}} + \mu_X\right)\right] = \alpha \tag{6}$$

Confidence interval for the mean is given by

$$\left[\overline{X} - \frac{\sigma_X\, \eta_{\alpha/2}}{\sqrt{N}} \le \mu_X < \frac{\sigma_X\, \eta_{\alpha/2}}{\sqrt{N}} + \overline{X}\right] \tag{7}$$

at a confidence level 100(1-α)%

3.3.5.2 Distribution of the Sample Variance

$$s^2 = \frac{1}{N-1}\sum_{i=1}^{N}\left(X_i - \overline{X}\right)^2 \tag{8}$$

For a normally distributed X the distribution of s^2 is a **Chi-Square Distribution,** χ^2_n, with n = N-1 degrees of freedom.

$$\text{Probability}\left[s^2 > \left(\frac{\sigma_X^2 \chi^2_{n;\alpha}}{n}\right)\right] = \alpha \tag{9}$$

confidence interval for the variance:

$\left[\frac{s^2 n}{\chi^2_{n;\alpha/2}} \le \sigma_X^2 < \frac{s^2 n}{\chi^2_{n;1-\alpha/2}}\right]$ at a confidence level 100(1-α)% with n= N-1.

3.3.5.3 Distribution of the Sample Mean When the Variance Is Unknown

For a normally distributed X the distribution of $\overline{X}$ is a **Student-t distribution,** t_n, with n = N-1 degrees of freedom.

$$\text{Probability}\left[\overline{X} > \left(\frac{st_{n;\alpha}}{\sqrt{N}} + \mu_X\right)\right] = \alpha \tag{10}$$

Confidence interval for the mean:

$$\left[\overline{X} - \frac{\sigma_X\, t_{n;\alpha/2}}{\sqrt{N}} \leq \mu_X < \frac{\sigma_X\, t_{n;\alpha/2}}{\sqrt{N}} + \overline{X}\right] \tag{11}$$

at a confidence level 100(1-α)% with n = N-1.

Using the Student-t distribution definition given above, the data obtained from different measurement methods is characterized to determine the tolerance limits for different manufacturing methods at a given confidence level.

Some of the SEM images with measurements and tolerance limits at a confidence level of 95% are given below.

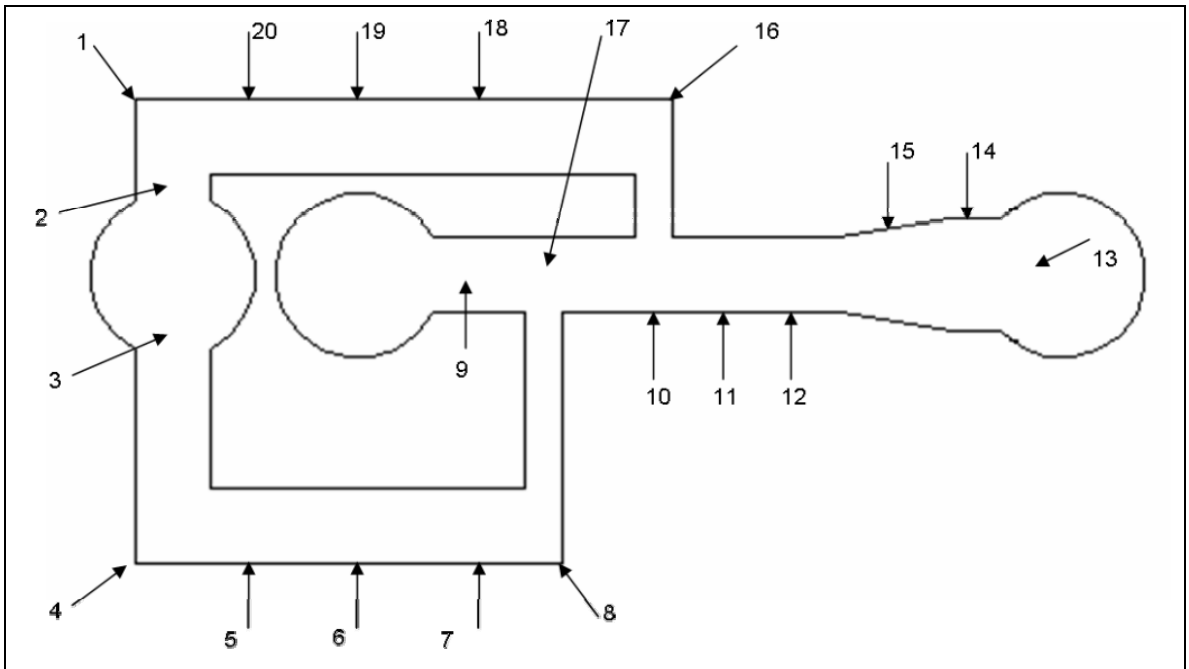

Figure 3.5 Jets in Cross Flow Mixer(X2J) with 1mm offset inlet jets designed dimensions Jet inlet width is 12.5µm, and channel width 25µm. Designed height of mixer 150µm

Figure 3.5 gives different locations on the mixer design where measurements are taken on

the mold insert and embossed PMMA chip. On mold insert, these measurements are taken by stylus profilometer and also from SEM images at the same locations. For PMMA embossed chips, the measurements are taken only from the SEM images.

SEM Images of the Brass Mold Insert

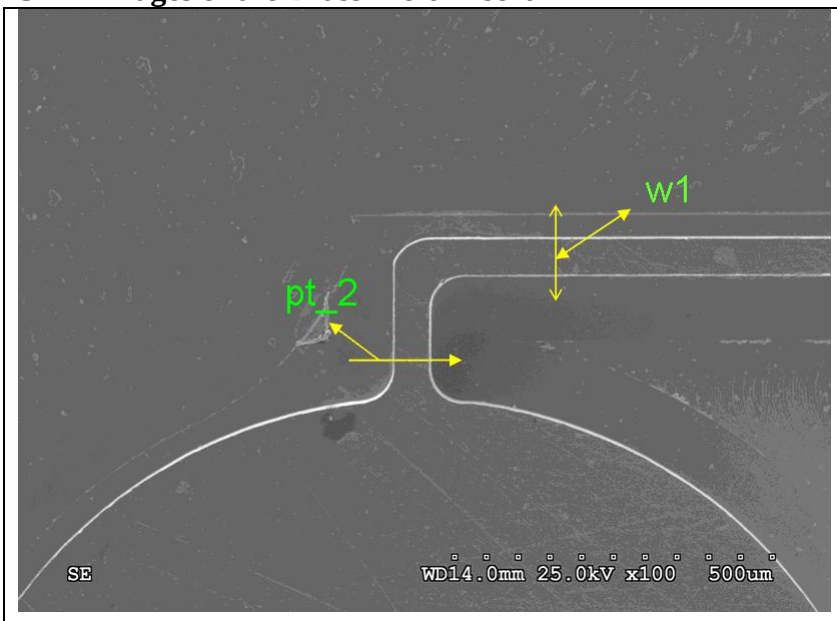

Figure 3.6 X2J mixer 1st Reservoir(for side jets) with rounded corners

average width w1 = 53.01µm +/- 0.90

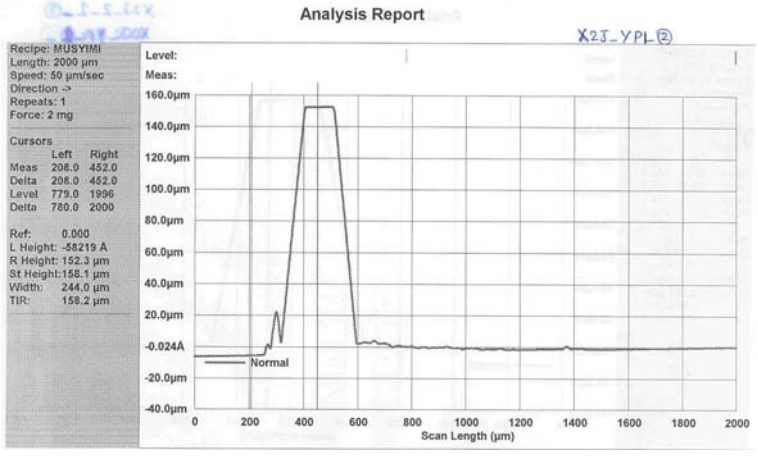

Figure 3.7 X2J mixer profilometer height measured at pt_2

average St. Height from profilometer =158.1µm (measured at pt_2 indicated above in SEM image)

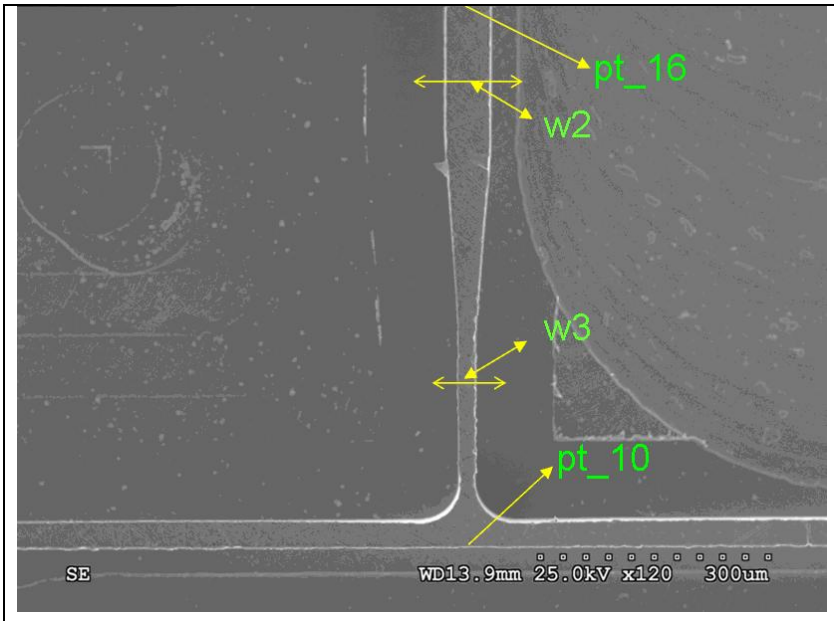

Figure 3.8 X2J mixer 2nd inlet from top

average width
w2 = 53.07µm +/- 0.71
(before jet contraction)

average width
w3 = 18.64µm +/- 0.565
(after jet contraction)

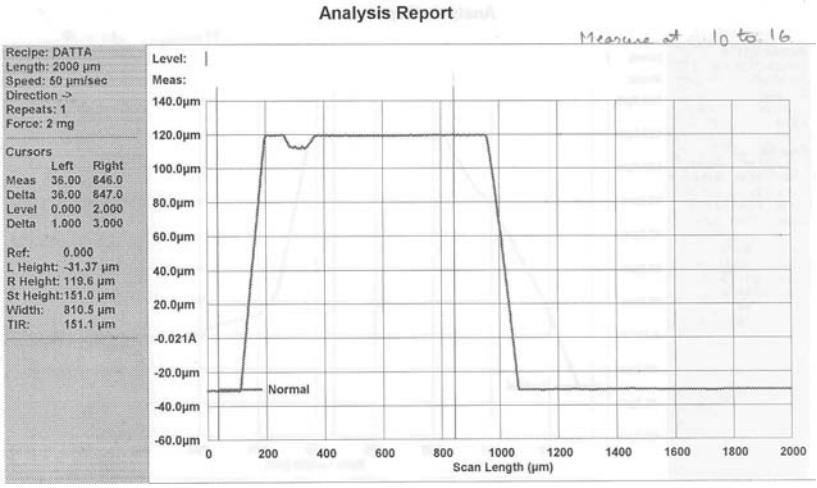

Figure 3.9 X2J mixer profilometer height measured from points pt_10 to pt_16

average height from profilometer = 151µm

Measurements on the image at different locations are made using the scion image software and using the Student-t distribution, the tolerance values of the measurements interval are calculated at a confidence level of 95 percentile and are compared with the design values. These values are displayed in the table 3.2

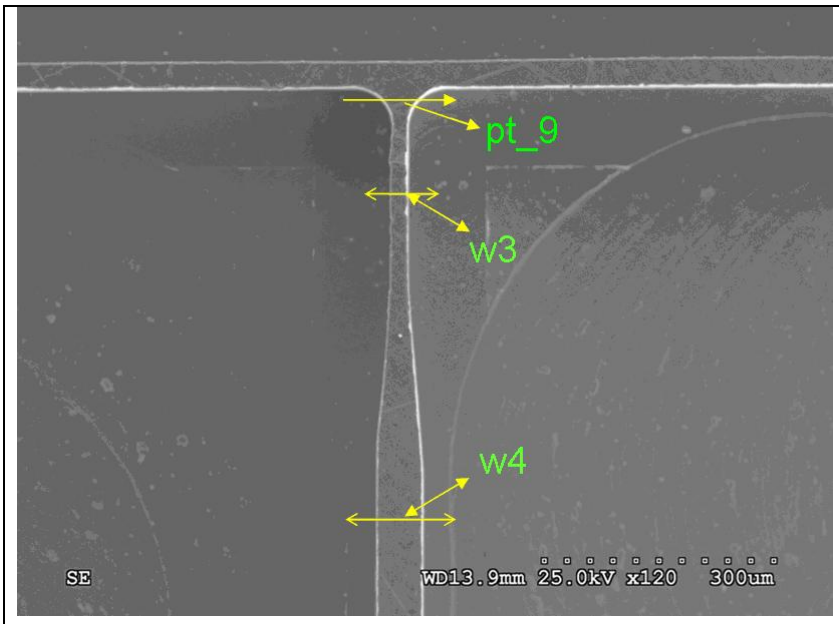

Figure 3.10 X2J mixer 1st inlet from bottom

average width
w3 = 14.54µm +/- 0.876
(after jet contraction)

average width
w4 = 51.32µm +/-1.04
(before jet contraction)

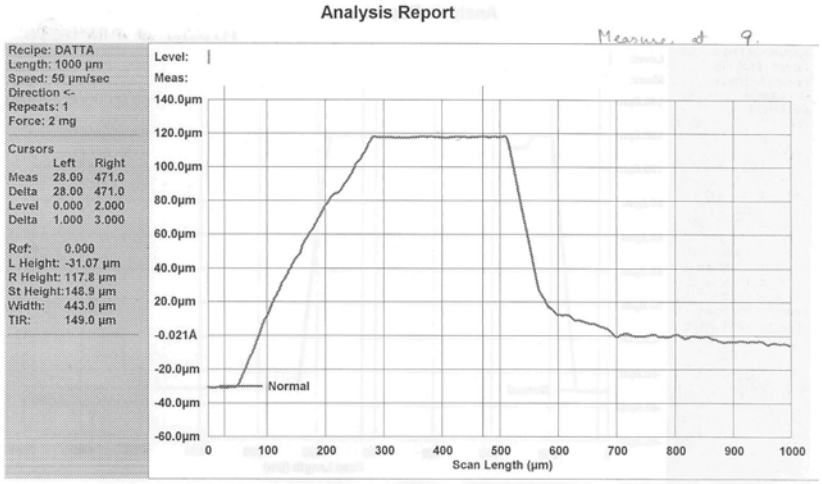

Figure 3.11 X2J mixer 1st inlet profilometer height measured at pt_9

average height from profilometer = 148.9µm

The profilometer analysis report from figure 3.11 shows the profile of the tapered stylus that is run on the mold insert at pt_9, which is not straight due to the radius of the stylus and the tapered shank. The feature height is given as the average of couple of runs of the profilometer at the same location.

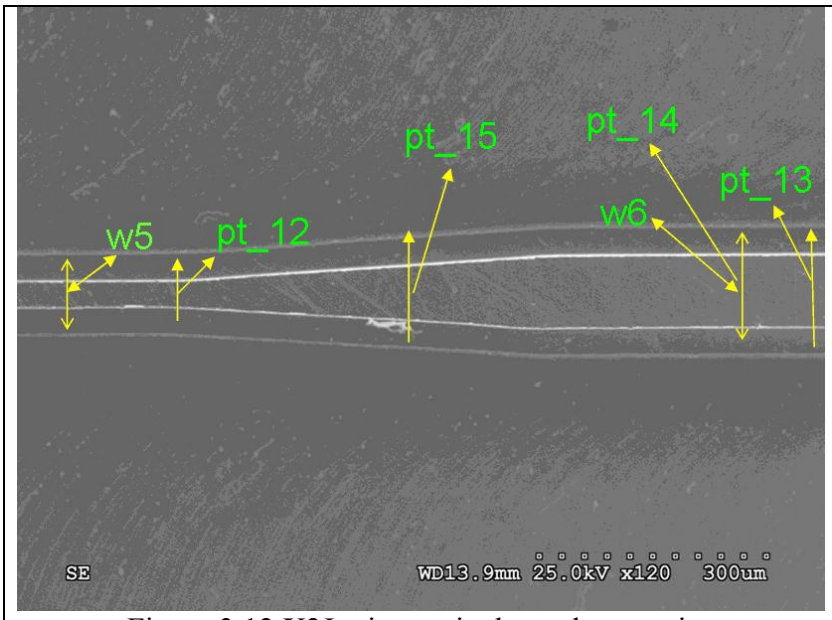

average width
w5 = 29.95+/- 1.435
(before channel expansion)

average width
w6 = 88.98 +/- 1.43
(after channel expansion)

average height from profilometer = 151µm

Figure 3.12 X2J mixer exit channel expansion

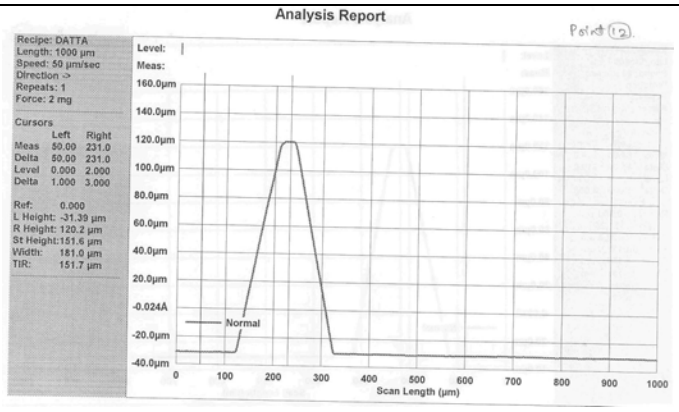

Figure 3.13 Height from profilometer measured on mold insert at point 12 (pt_12) 151.6µm

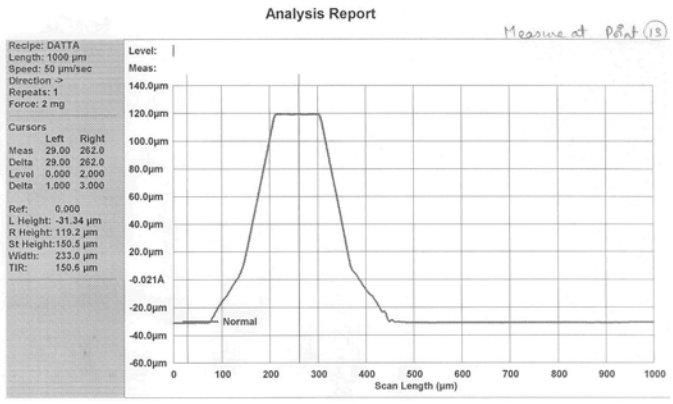

Figure 3.14 Height from profilometer measured on Mold Insert (MI) at point 13 (pt_13) 150.5µm

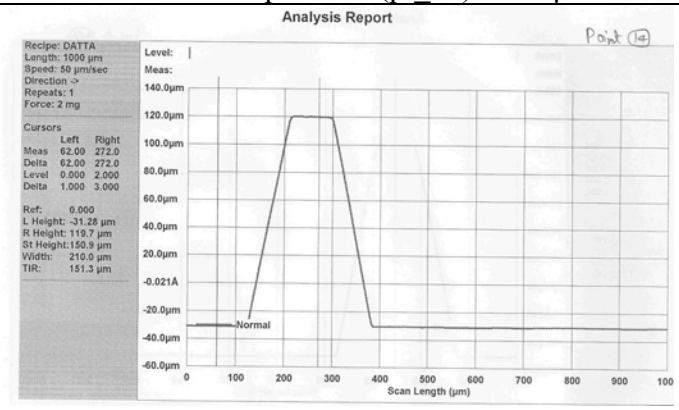

Figure 3.15 Height measured using Profilometer on Mold insert at point 14 (pt_14) 150.9µm

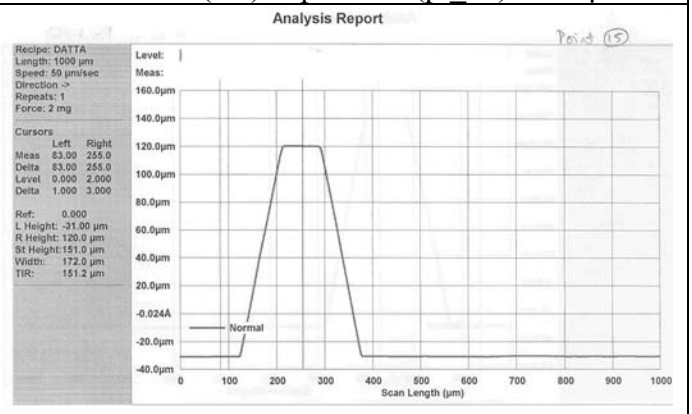

Figure 3.16 Height measured using Profilometer on Mold insert at point 15 (pt_15) 151µm

SEM Images of Embossed PMMA chip

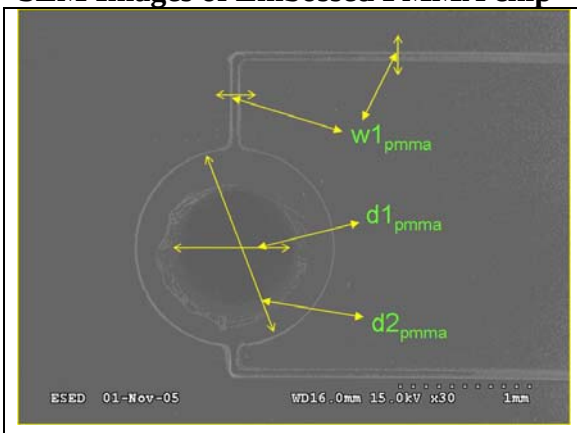

Figure 3.17 X2J PMMA Reservoir 1

Average width of channel
$w1_{pmma}$=36.665 +/- 3.83µm.

Diameter of
drilled hole
$d1_{pmma}$ = 958.83 +/- 6.77 µm.

Average diameter
of reservoir is
$d2_{pmma}$ = 1485.92 +/- 6.24µm.

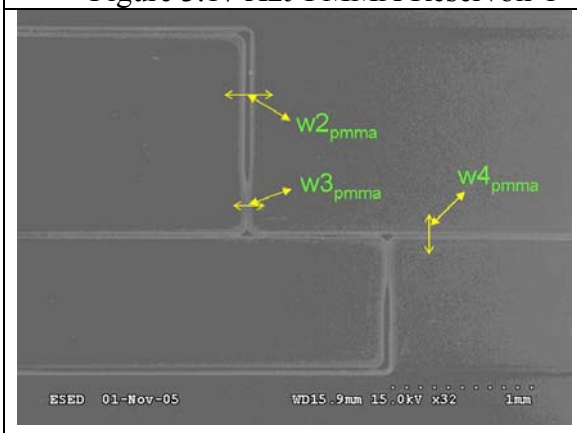

Figure 3.18 X2J PMMA Inlet jets

Average width
(before contraction)
$w2_{pmma}$ = 28.1 +/- 3.25µm

Average width
(after contraction)
$w3_{pmma}$ = 12.42 +/- 0.5µm

Average width of mixing channel
$w4_{pmma}$ = 31.06 +/- 0.7µm

Table 3.2 Comparing design and measured dimensions

width at reservoir, w1	Design – 50 µm Mold Insert – 53 +/- 1µm PMMA – 36.6 +/- 4µm
Diameter of ports, d2	Design – 1500µm Mold Insert – 1548 +/- 10µm PMMA – 1486 +/- 6µm
width of mixing channel, w5	Design – 25µm Mold Insert – 29.9 +/- 2µm PMMA – 21.3 +/- 1µm
Feature Height	Design - 150µm Mold Insert – 155.3 +/- 5µm PMMA – 142.5 +/- 4µm

Table 3.2 compares some of the measured dimensions of jets in cross flow mixer with 1mm offset between jets with those of design dimensions. The feature height on embossed PMMA chips are measured values using the microscope.

SEM images of brass mold insert compared with those of PMMA embossed chips

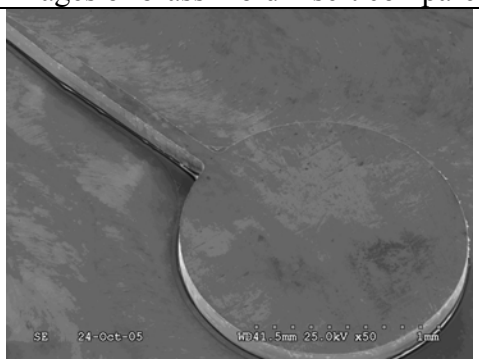

Figure 3.19 Exit port on Mold Insert

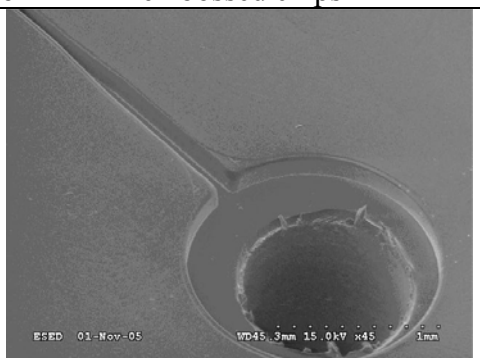

Figure 3.20 Exit port on PMMA

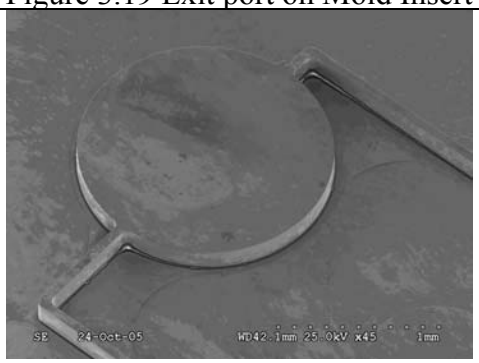

Figure 3.21 First Reservoir on Mold Insert

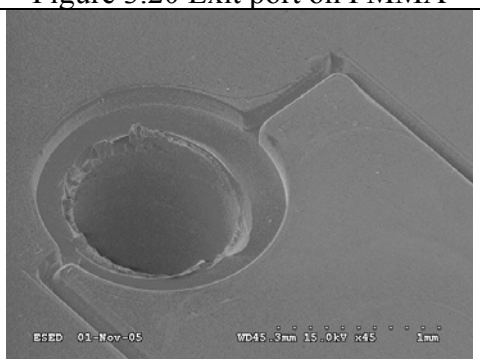

Figure 3.22 Embossed Reservoir with hole

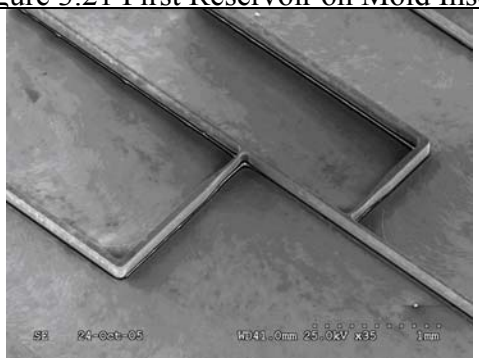

Figure 3.23 Jets in Cross Flow with an offset

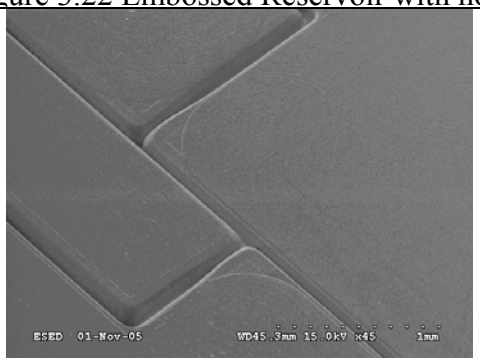

Figure 3.24 Embossed channels in PMMA

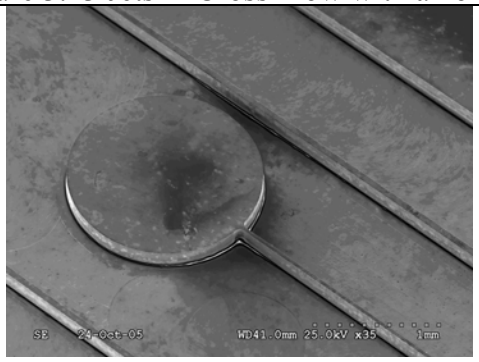

Figure 3.25 Second Reservoir

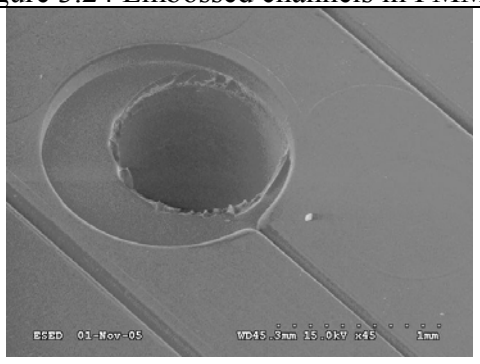

Figure 3.26 Embossed and Drilled Reservoir

Micro milled brass mold insert is used to hot-emboss into polymethylmethacrylate to obtain micro-mixers which are covered and are used for experiments. The metrology gives us the tolerances which can be expected during manufacturing of micro-mixers using the methodology described in this chapter. Measurement of embossed PMMA chips using destructive measurement produced burs on the edges of the chip width and the actual dimensioning of the chip with this method is not available. A measurement of the same embossed chip at different locations was made using the microscope for the depth of the channel and is reported. The tolerance values obtained can thus be used to modify the design dimensions to achieve the actual dimensions that are used for experimentation.

Chapter4. Simulations and Experiments

4.1 Mixer Designs

As discussed in the earlier chapter the jets in cross flow mixer, designed and developed by Maha *et.al* is used for our current study. The jets in cross flow mixers with no offset and 1mm offset are meshed with equally spaced grid to perform some more simulations using fluent.

4.2 Optimal Flow Ratio in a Three Layered Micro-Mixer

Based on the theory discussed in chapter 2, the optimum individual flow rates and flow rate ratio can be estimated using the semi-analytical theoretical solution for laminar flow in rectangular channels as given in [White, F.M., 1974, "Viscous Fluid Flow". Figure 2.2 shows the dependence of the optimum flow rate ratio, $\psi_{o,}$ on the channel aspect ratio for various multi-stream micro-mixers. As the number of mixing streams increases the sensitivity of ψ_o with aspect ratio is reduced. Considering our current case with jets in cross flow, mixer having three jets coming in contact (one main and two side jets), a three layer mixer, the optimum value of ψ_o for channels with aspect ratios of three and above as given in literature is 2.18 ~ 2.2. Simulations are run on jets in cross flow mixer with no offset for varying flow ratios of 1:1, 1:10, 10:1, and 2.18:1. The results are plotted for different efficiencies to define the optimum flow rate ratio in order to minimize the total mixture production time and also the length of the mixing channel.

Flow ratio in our current simulation cases is defined as ratio of flow rate of fluid flowing in main channel to that flowing in the side jets. Water is taken as the fluid flowing in the center and DNA or the second reagent is taken to be flowing in the side

jets in the simulations. All the properties of the water are also applied to DNA. Concentration of water is taken as zero and that of DNA as $1.44X10^{-6}$ M.

4.3 Numerical Simulation Using Fluent 5.4

Fluent 5.4 and 6.1.2 solvers are used on parallel network to perform numerical simulations for different flow ratios on the jets in cross flow mixer design to verify the above analysis. The mixer is re-designed based on the dimensions of Maha (2005) and meshed uniformly using hexahedral elements. These channels were meshed using hexahedral elements. Dense mesh is used for these simulations to avoid numerical error in the simulation results. A diffusion coefficient of 1.2×10^{-10} m^2/s is used for these simulations, which is similar to the reagents used in the Polymerase Chain Reaction (PCR) devices. The mixer design is uniformly meshed at all locations, including the corners and edges of the straight channels. Designed dimensions used for manufacturing were used for current numerical simulations. These geometries are symmetrical over half their depth which enabled to incorporate a refined and dense mesh for numerical analysis. The width, depth, and length for these designs correspond to x, y, and z coordinates respectively.

Maha (2005) in his thesis describes the governing equations that are solved by Fluent. It solves for equations of mass, momentum and energy for all fluid flows and also solves for species conservation equation for flows involving mixing of two or more reagents. The conservation of mass or continuity equation can be written as

$$\frac{\partial \rho}{\partial t} + \frac{\partial}{\partial x_i}(\rho u_i) = 0 \qquad (12)$$

In an inertial (non-accelerating) reference frame the conservation of momentum is given by

$$\frac{\partial}{\partial t}(\rho u_i) + \frac{\partial}{\partial x_i}(\rho u_i u_j) = -\frac{\partial p}{\partial x_i} + \frac{\partial \tau_{ij}}{\partial x_j} + \rho g_i + F_i \tag{13}$$

The last two terms on the right hand side of the equation ρg_i and F_i denote the gravitational and external body forces respectively. p is the static pressure and τ_{ij} is the stress tensor given by

$$\tau_{ij} = \left[\mu \left(\frac{\partial u_i}{\partial x_j} + \frac{\partial u_j}{\partial x_i} \right) \right] - \frac{2}{3} \mu \frac{\partial u_l}{\partial x_l} \delta_{ij} \tag{14}$$

where μ is the molecular viscosity and second term on right hand side of the above equation is due to volume dilation. The multi component diffusion energy equation is solved in fluent in the form of

$$\frac{\partial}{\partial t}(\rho Y_i) + \nabla \cdot (\rho \vec{v} Y_i) = -\nabla \cdot \vec{J}_i + R_i + S_i \tag{15}$$

Y_i the local mass fraction for the *i*th species, R_i is the net rate of production of species *i* by chemical reaction and S_i the rate of creation by addition from a dispersed phase plus any user defined sources. Above equation is solved for N-1 species where N is the total fluid phase chemical species present in system. D_{ij} is the diffusion flux of species *I*, arising due to concentration gradients. In the case of multi-component systems, it is not possible to derive relations for diffusion fluxes containing a gradient of only one component. For diffusive mass flux, Maxwell-Stefan equations are used.

$$\sum_{\substack{j=1 \\ j \neq i}}^{N} \frac{X_i X_j}{D_{ij}} \left(\vec{V}_j - \vec{V}_i \right) = \vec{d}_i - \frac{\nabla T}{T} \sum_{\substack{j=1 \\ j \neq i}}^{N} \frac{X_i X_j}{D_{ij}} \left(\frac{D_{T,j}}{\rho_j} - \frac{D_{T,i}}{\rho_i} \right) \tag{16}$$

where X is the mole fraction, $\vec{V}$ is the diffusion velocity. D_{ij}, D_T being the binary diffusion coefficient and thermal diffusion coefficient respectively.

4.4 Numerical Simulation Results

4.4.1 Mixing Efficiency of Micro-Mixer

The mixing efficiency introduced by Erickson D. and Li D. (2002) for evaluation of their mixers is given by

$$\varepsilon = \left(1 - \frac{\frac{1}{A_e}\int_{A_e} |c - c_\infty| dA}{\sum_i \frac{1}{A_i}\int_{A_i} |c_i - c_\infty| dA} \right) \cdot 100\% \qquad (17)$$

where, A_e is the area of the exit, A_i is the area of the inlet, c the local concentration, c_i the concentration at the i^{th} inlet and c_∞ is the infinite fully mixed concentration. This definition is applicable when efficiency is being evaluated locally for a micro-mixer; unlike in the case of batch production mixers the important aspect to be considered is the rate of production of the mixed product at the exit of the micro-mixer. For which, Maha *et. al.,* introduced the following definition.

$$\eta = \left(1 - \frac{\int_{A_e} \rho_e V_e |c_e - c_\infty| dA}{\sum_i \int_{A_i} \rho_i V_i |c_i - c_\infty| dA} \right) \cdot 100\% \qquad (18)$$

where, c_e, V_e, ρ_e are the concentration, velocity and density at the exit port of the mixer (of the mixed product) while c_i, V_i, and ρ_i are those at the inlets. This definition of mixer efficiency is applicable for the case when the flow ratio ψ_o is 1:1, ie., for cases where the flow rate in the main stream channel is equal in proportion to that in the side jets. For

cases involving different flow ratios as discussed in chapter 2, the efficiency of the mixer is evaluated for different definitions which are defined as follows.

4.4.2 Different Definitions

Mixer efficiency is calculated based on different definitions which are based on the parameters involved with the mixing fluids, like the flow rate, concentration of the fluids before mixing, infinite concentration, concentration at a particular location in the mixing channel, total area of the chamber, etc. These different definitions are listed with their formula described as in the FORTRAN code given in Appendix A.

1. $$efc\inf\ pos\,(Eff\ C_{\infty}\ Pos) = \left(1 - \frac{\sqrt{(C - C_{\infty})^2}}{\psi * 100}\right) * 100 \tag{19}$$

2. $$efc\inf neg(\ Eff\ C_{\infty}\ Neg) = \left(1 - \frac{\sqrt{(C - C_{\infty})^2}}{100}\right) * 100 \tag{20}$$

3. $$efc\inf = (efc\inf pos * dA / Atot) + (efc\inf neg * dA / Atot) \tag{21}$$

4. $$efc\inf ABSpos = \left(1 - ABScc\inf pos / (florat * 100)\right) * 100 \tag{22}$$

5. $$efc\inf ABSneg = \left(1 - ABScc\inf neg / (100)\right) * 100 \tag{23}$$

6. $$efc\inf\ ABS = (efc\inf\ ABSpos * dA / Atot) + (efc\inf\ ABSneg * dA / Atot) \tag{24}$$

7. $$efRMSQc\inf = 1 - RMSQcc\inf / RMSQcc\inf 0) * 100 \tag{25}$$

8. $$efABSQc\inf = 1 - ABSQcc\inf / ABSQcc\inf 0) * 100 \tag{26}$$

9. $$\boxed{efABSc\inf = (1 - ABScc\inf / ABScc\inf 0) * 100 = 1 - \frac{\frac{1}{A}\int |C - C_{\infty}| dA}{\left[\frac{1}{A}\int |C - C_{\infty}| dA\right]_{1stplane}}} \tag{27}$$

10. $$efABScA = (1 - ABSccA / ABSccA0) * 100 \tag{28}$$

4.4.3 Jets in Cross Flow

Numerical simulations have been performed by Maha (2005) on different mixer designs and are presented in his thesis. As discussed in the previous chapters, this particular design consists of a straight middle channel of aspect ratio of about 6 and two channels of twice the aspect ratio entering into the mixing channel at right angles. From the numerical and experimental data of Maha, this design was shown to perform best with a mixing efficiency of 86% and an optimum pressure drop across the mixer. Additional simulations are performed on this design with refined and equally spaced grid for different flow ratios in the inlet channels to study the effect of flow-ratio variation on the mixing performance, total mixture production time and pressure drop.

4.4.3.1 Flow Ratio 1:1

The design has a main straight channel of width 25μm, extending for a length of 712.5μm, and two side jets at right angles to the main channel from side at about 200μm from the first inlet. The width of the side jets is about 12.5μm. The mixer has a uniform height of about 150μm. Direction of flow of fluid is taken as z-axis, x-axis along the width of the channel, and y-axis extending along the height of the mixer. It is symmetrical about two planes, x-z plane extending along the mixer height and y-z plane along mid-way of the mixing channel width. The total number of nodes for the simulation of this mixer design with jets in cross flow with no off-set was about 3,850,000. As defined earlier in Chapter 2, flow ratio is the ratio of sum of all even inlets to the sum of all odd inlet flow rates. In this particular case we have 3 inlets, first from the top $Q_{s/2}$, second from the center Q_c and third from the bottom $Q_{s/2}$. From the geometry we can see

$$Q_{s/2} + Q_c + Q_{s/2} = Q_T \quad (19)$$

Total flow rate, Q_T used for simulation is 26.34nL/s (value based on calculations for optimum flow rate which in turn depends on channel dimensions and aspect ratio). For a flow ratio of 1:1, this would split up as flow in side jet. $Q_{s/2}$ = 6.585nL/s, and flow in center channel, Q_c = 13.17nL/s. The results of the simulation are shown in the images given below.

The flow contours for 1:1 flow ratio are shown below.

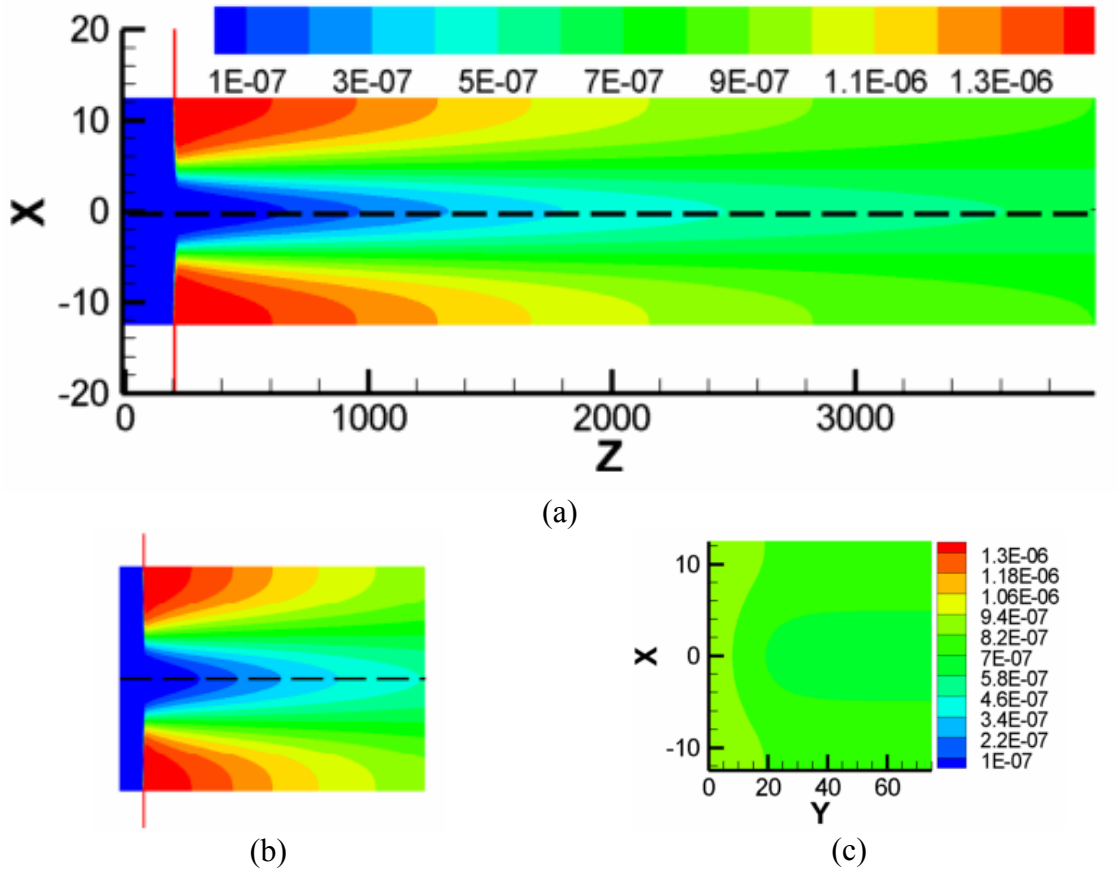

Figure 4.1 Mixing of Jets in Cross Flow for a flow ratio of 1:1
(a) Top view of x-z plane along the center of mixer.
(b) 3-Inlets start mixing: concentration plane contours
(c) Exit plane concentration contours (75μm, half channel depth)

4.4.3.2 Flow Ratio 1:10

Total flow rate Q_T equal to 26.34nL/s and flow rate ratio 1:10 for jets in cross flow mixer.

Total Flow rate, Q_T = 26.34nL/s. We know from equation (19),

$$Q_c + Q_s = Q_T, \text{ and}$$

$$Q_c / Q_s = 1/10$$

we get from the above two equations, Q_c = 2.3945nL/s, and Q_s = 23.945nL/s.

The flow contours for 1:10 flow ratio are shown below.

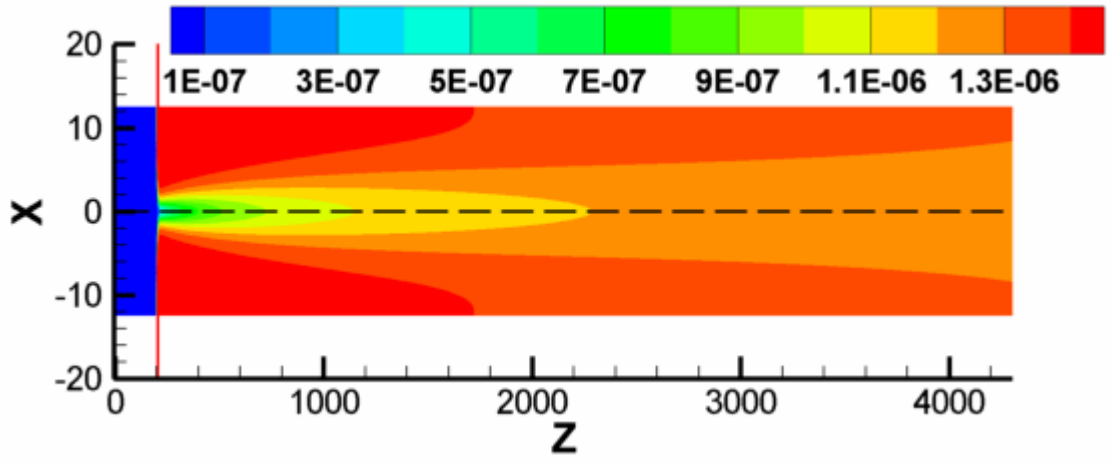

(a)

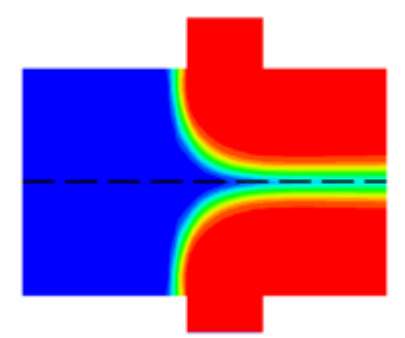

(b)

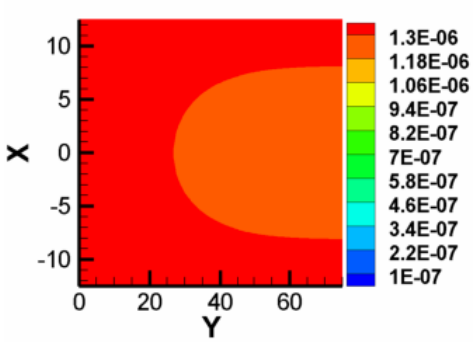

(c)

Figure 4.2 Mixing of Jets in cross flow for a flow ratio of 1:10
(a) Top view of x-z plane along the center of mixer.
(b) 3-Inlets start mixing: concentration plane contours
(c) Exit plane concentration contours (75µm,half channel depth)

4.4.3.3 Flow Ratio 10:1

Total flow rate Q_T equal to 26.34nL/s and flow ratio 10:1 mixing in jets in cross flow mixer.

Total Flow rate, Q_T = 26.34nL/s. We know from equation (19),

$$Q_c + Q_s = Q_T, \text{ and}$$

$$Q_c / Q_s = 10/1$$

we get from the above two equations, Q_c = 23.945nL/s, and Q_s = 2.3945nL/s.

The flow contours for 10:1 flow ratio are shown below.

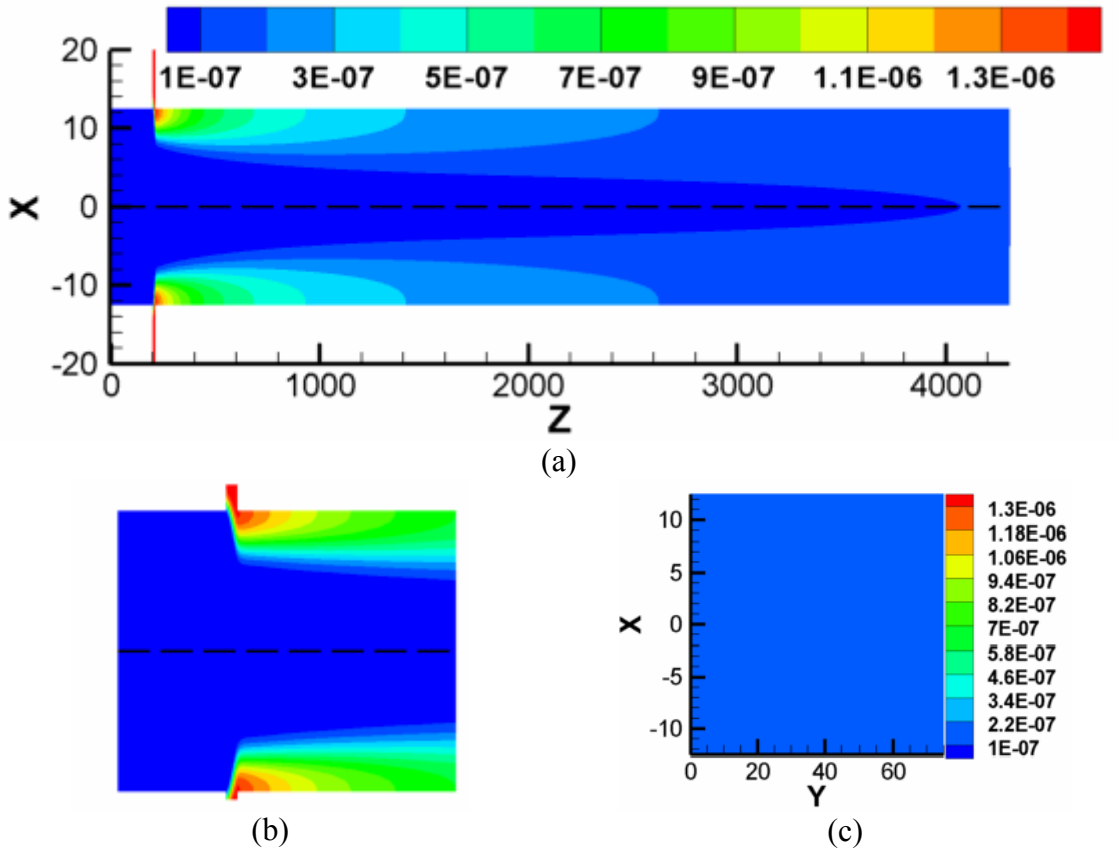

Figure 4.3 Mixing of Jets in cross flow for a flow ratio of 10:1
(a) Top view of x-z plane along the center of mixer.
(b) 3-Inlets start mixing: concentration plane contours
(c) Exit plane concentration contours (75µm,half channel depth)

4.4.3.4 Flow Ratio 2.18:1

Total flow rate Q_T equal to 26.34nL/s and flow ratio 2.18:1 mixing in jets in cross flow mixer.

Total Flow rate, Q_T = 26.34nL/s. We know from equation (19),

$$Q_c + Q_s = Q_T, \text{ and}$$

$$Q_c / Q_s = 2.18/1$$

we get from the above two equations, Q_c = 18.05694nL/s, and Q_s = 8.283nL/s.

The flow contours for 2.18:1 flow ratio are shown below.

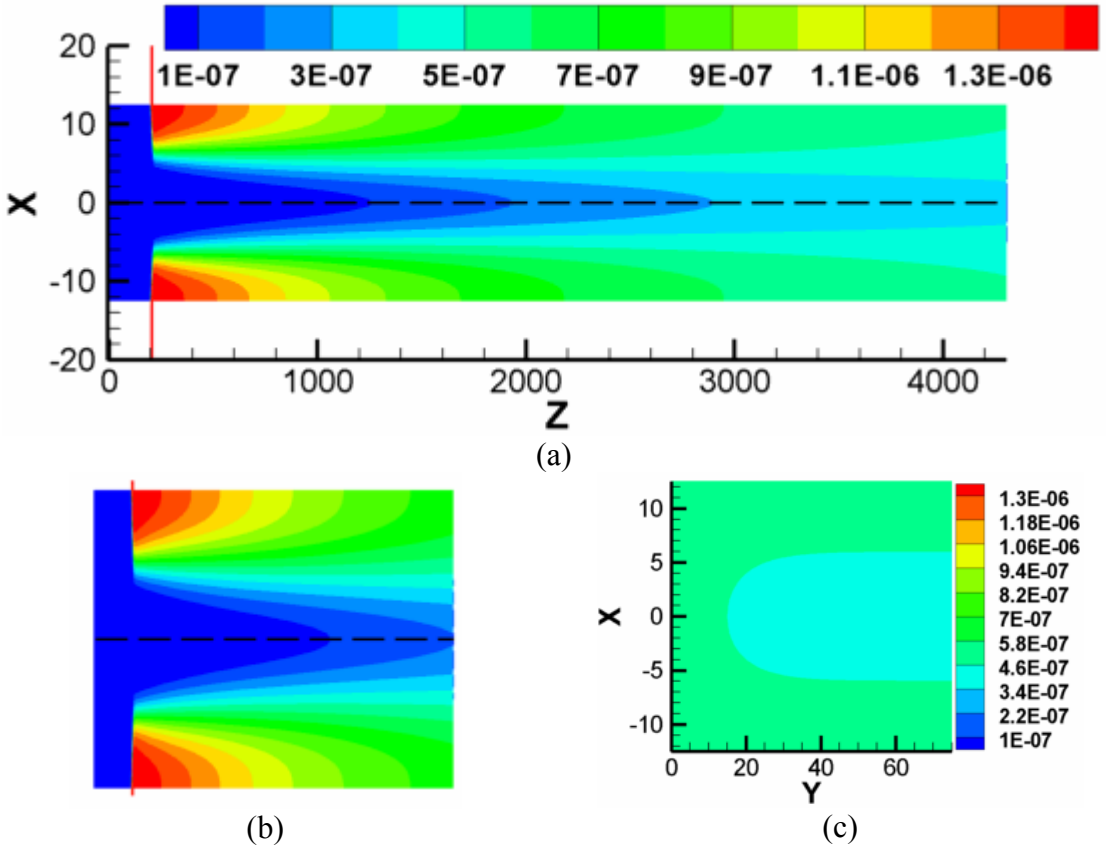

Figure 4.4 Mixing of Jets in cross flow for a flow ratio of 2.18:1
(a) Top view of x-z plane along the center of mixer.
(b) 3-Inlets start mixing: concentration plane contours
(c) Exit plane concentration contours (75µm,half channel depth)

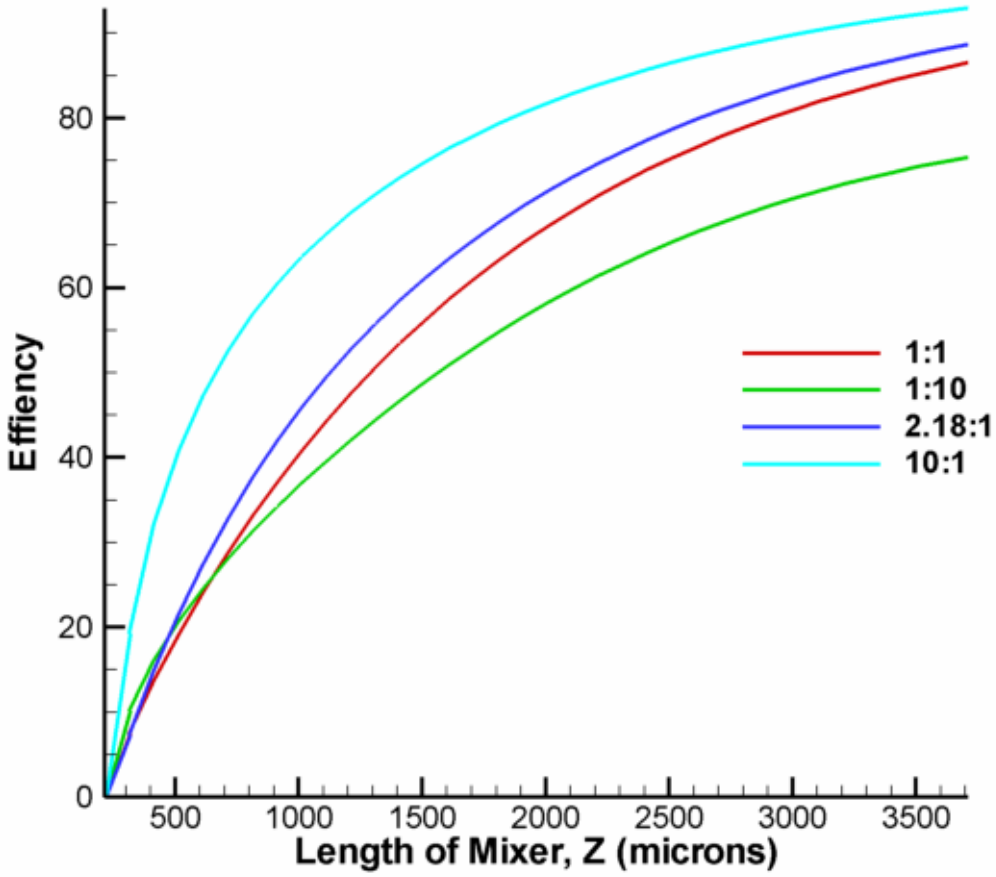

Figure 4.5 Mixing efficiencies based on Equation (27) for jets in cross flow mixer with no offset and with different flow ratios

Slices are taken along the length of the mixing channel right after the two side jets meet the jet in the main channel, in the z-direction and efficiencies are calculated based on the different definitions described in section 4.4.2, and are plotted for Equation (27) which compares the mixed efficiency at the exit of the mixer with that of the efficiency of first plane at the mixing channel. These efficiencies for different flow ratios are compared in the plot shown in Figure 4.5. X-axis represents the length along the mixer in microns starting from the junction where the main jet and two side jets meet in the mixing

channel, while the Y-axis represents the efficiency calculated using equation (27). As seen from the Figure 4.5, higher effiency curve along the length of the mixer can be found for a 10:1 flow ratio and then 2.18:1 flow and then the 1:1 and 1:10 follow. Higher effiency in case of 10:1 when compared to 2.18:1 can be explained due to the three dimensional effects occurring at the junction where all the three jets meet in the mixing channel and start mixing. The 2.18:1 flow ratio shows better mixing efficiency than the 1:1 and 1:10 flow ratio for the jets in cross flow mixer with no offset between the side jets.

4.4.4 Jets in Cross Flow with an Offset

Simulations are performed on jets in cross flow mixer with side jets placed at an offset of 1mm for different flow ratios as in the previous case. The simulation results for the coarse grid are compared with the experimental results of mixing on jets in cross flow mixer with an offset. Different dimensions of the jets in cross flow mixer with an offset are given in Appendix C. A total flow ratio of 26.34nL/s is maintained for these simulations. Concentration of Rhodamine B dye is taken as 1.44E-06 while a value of zero assigned for water and simulation is run under steady state conditions. Figure 4.6 shows the contour plots for different flow ratios in jets in cross flow with jets placed at an offset of one millimeter.

Figure 4.7 shows the plot for efficiency on Y-axis against the length of the mixer in microns along X-axis. The initial behavior of curves before a Z value of 1100, can be taken as a two stream mixer with first stream in main channel and the second one entering from the side jet. The second side jet has not yet entered at this Z location.

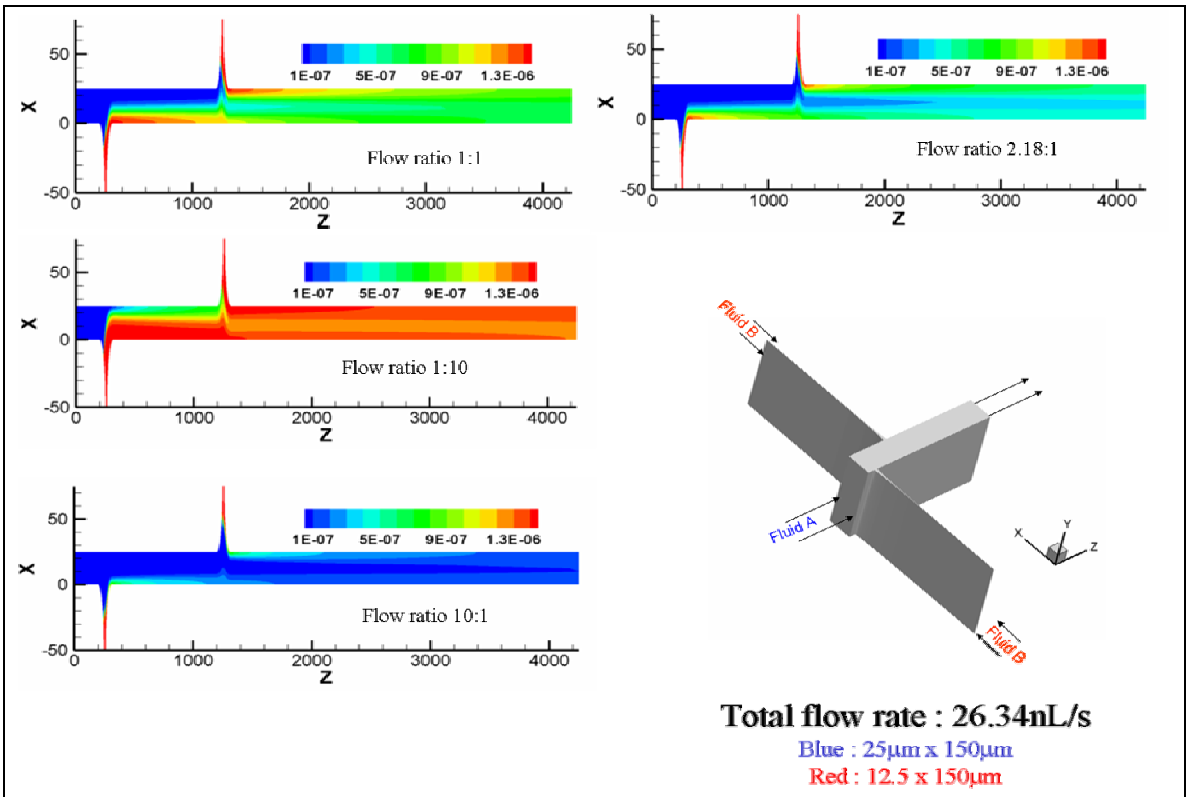

Figure 4.6 Concentration contour plots for different flow ratios along the length of the mixer for jets in cross flow mixer with an offset of 1mm

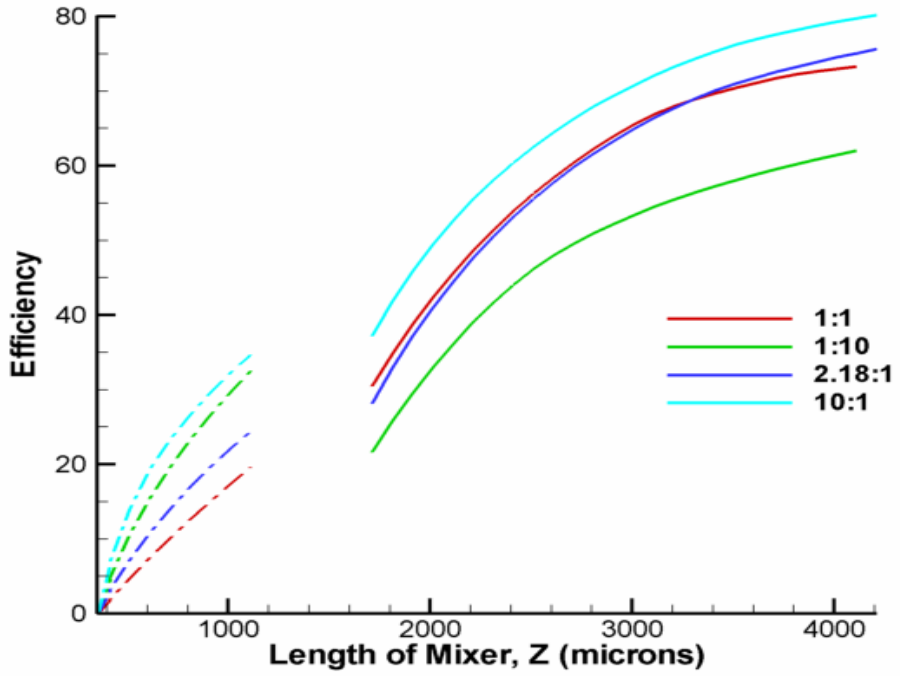

Figure 4.7 Mixing efficiencies for jets in cross flow mixer with an offset of 1mm for different flow ratios.

The plots show that there is an increased efficiency by varying the flow rate ratio. After the second jet is introduced into the mixing channel, the mixing behavior similar to that observed in a three stream jets in cross flow mixer with no offset as described in previous section. The efficiency curve for a flow rate ratio of 2.2 is found to be higher than 1:1 and 1:10 flow rates while the higher efficiency curve for a 10:1 flow can be explained due to the three dimensional effects occurring at the junction where the three jets meet in the mixing channel. Due to entrapment of the fluid in the middle, which is due to higher flow rates at the boundary for a ten to one flow ratio, higher mixing can be observed locally at that particular location. Experimental verification of the same can checked to verify the results of the simulation for a jets in cross with jets placed at an offset. Also by measuring the mixture production time, optimum mixer length required to produce a specific volume of mixed product, we can compare between flow ratios to get an optimum flow rate to be used for better mixing.

4.5 Experimental Setup

An Olympus IX70, inverted epi- fluorescent microscope was used for performing experiments on jets in cross flow micro-mixer with an offset of 1mm and having rounded corners. Bejat (2001), and Maha (2005) in their thesis describe in detail about various components of the microscope. The microscope stage H107 with a resolution of ±1μm from PRIOR Scientific is used which can be controlled manually using a joystick and also by a PC with a RS232 connection. Light source used for the experiments was a continuously illuminated mercury lamp which provided broadband spectrum. A filter set designed for samples having green light excitation (U-MWIG2-Olympus) is used in our mixing experiment with Rhodamine B fluorescent dye (excitation – 546nm, emission –

590nm) solution and de-ionized water. The microscope has an optical filter assembly that directs the light beam from the source to the objective lens. The objective lens relays this light on to the micro-mixer chip illuminating the entire flow volume.

4.5.1 Schematic of Experimental Setup

As explained in Chapter 3, cleaned chip after thermally bonded with PMMA cover slip of 125μm thickness is used for the mixing experiments using Rhodamine B fluorescent dye solution. A plastic adapter is glued on the back side of the chip on the holes through which fluid is pumped into the micro channels using a syringe pump which has the capability to hold two syringes and push with the same velocity. It has in-built data regarding different types of syringes of different sizes and materials, or one can customize it with their own parameters. It can also be controlled with a PC using a RS232 connection to control the fluid flow. The micro-mixer is fixed in position without any relative movement between the chip and the stage using a plastic sheet and spring loaded screws. Images are captured using a CCD camera located beneath the microscope.

4.6 Experimental Results

4.6.1 Calibration Results

Previous experimental results done by Maha have shown that higher concentration Rhodamine B fluorescent solution ($1.44x10^{-5}M$) resulted in non-linear behavior between intensity distribution and concentration which was explained due to inner filter effects (decrease in emission quantum yield as a result of re-absorption of emitted radiation). Hence a new solution of lowest concentration from his experimental results was prepared and calibration experiments performed by preparing ten different solutions varying the concentration by 10% between them. Concentration range is

$1.44x10^{-6}M$ – $1.44x10^{-7}M$. Each solution is pumped into the micro-channel and images (80 images at each location) are taken at different locations starting from the first side jet on the micro channel by moving the microscope stage by 200μm until the second jet and

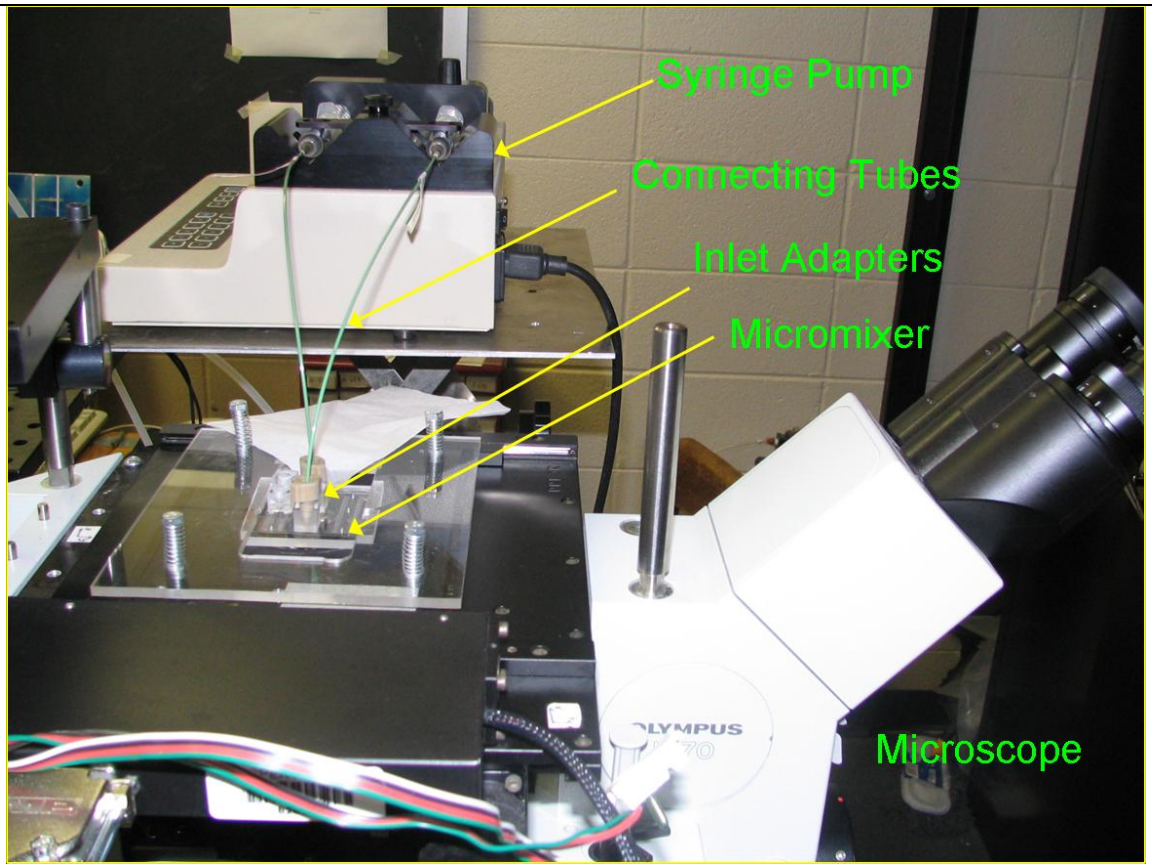

Figure 4.8 Experimental setup

some image sets in the mixing channel. Images are taken using a 40X air-immersion objective from Olympus using 4X4 binning on the pixels. Camera settings are maintained constant for all the images taken for different concentrations. These images are post-processed to plot the curve between average intensity of Rhodamine B solution and concentration variation (dilution). A linear variation between average intensity and dilution is found from the post processing results. Linear curve fit is plotted between the same and slope values from the equation are used in the Matlab code (taken from Appendix B of thesis by Maha-fall 2005) to estimate the efficiency in the mixing

experiment images. The same solution ($1.44x10^{-6}$M) is used for the mixing experiment using Rhodomine B fluorescent dye and di-ionized water running at different flow ratios.

Table 4.1: Camera conditions for Rhodamine B fluorescent dye intensity calibration with $1.44X10^{-6}$ M solution

Objective	Binning	Concentration (M)	%	Contrast	Brightness	Exp time (ms)
40X	4X4	1.44E-06	100	30	-50	0.5
		1.30E-06	90	30	-50	0.5
		1.15E-06	80	30	-50	0.5
		1.01E-06	70	30	-50	0.5
		8.64E-07	60	30	-50	0.5
		7.20E-07	50	30	-50	0.5
		5.76E-07	40	30	-50	0.5
		4.32E-07	30	30	-50	0.5
		2.88E-07	20	30	-50	0.5
		1.44E-07	10	30	-50	0.5

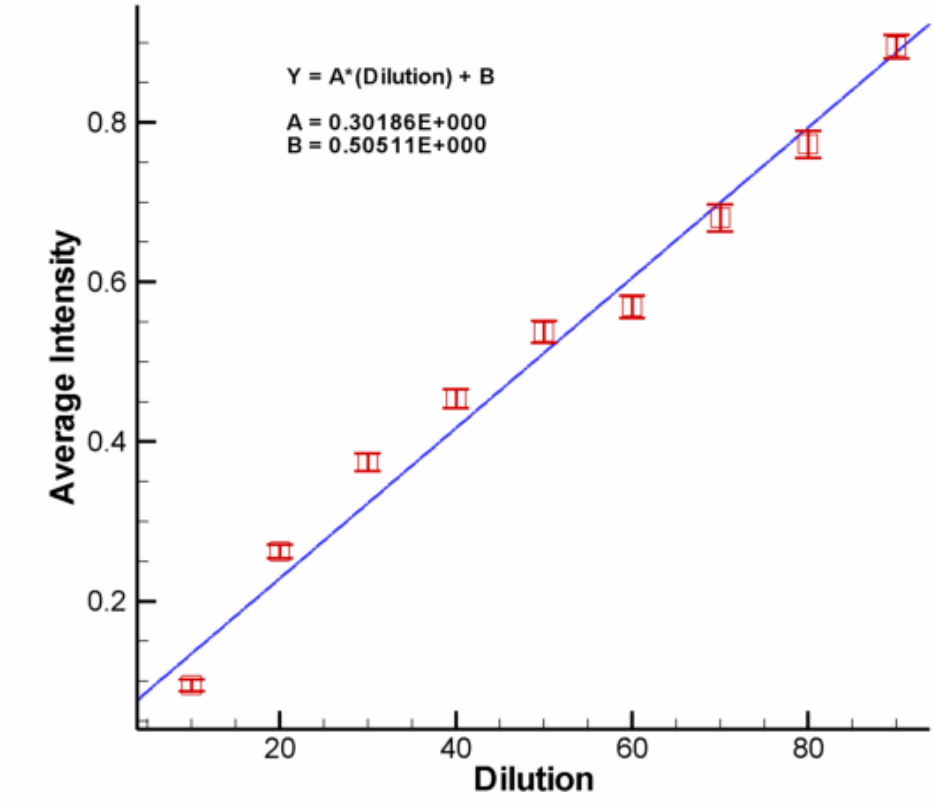

Figure 4.9 Intensity calibration curve for Rhodamine B fluorescent dye using $1.44X10^{-6}$ – $1.44X10^{-7}$ M solution

4.6.2 Rhodomine B Dilution Experiment with Different Flow Ratios

Mixing experiment is performed using Rhodamine B fluorescent dye and di-ionized water to compare the simulation results of the jets in cross flow with an offset for different flow ratios. These experiments are performed on the hot-embossed PMMA chip that has three mixers layered on a single chip as explained in previous chapters. As in simulation, Rhodamine is pumped through the side jets and di-water is pumped in the main center channel. Total flow rate used in experiments is same as that used in simulation at an optimum value of 26.34nL/s. To maintain different flow ratio in the mixing channels, we have two options. One, to use a combination of different diameter syringes which when pumped using equal linear velocity at the syringe pump would give us the required flow ratio of the mixing fluids. Second, to use different syringe pumps (New Era Syringe Pumps) which can be controlled with a PC. LabView is used as an interface to control these syringes with the PC. A VI (virtual instrument) developed by Estelle (thesis - fall 2006) to control these New Era single syringe pumps is used for experiments. Each syringe is set at an individual flow rate so as to maintain the flow ratio between the mixing fluid jets and also the total optimum flow ratio used for mixing. The fluorescence from the mixer was captured using a CCD camera, U-MWIG2 filter cube from Olympus and mercury lamp as source of light.

The PRIOR motorized stage was moved by 200μm and 100 frames of image sets are taken at each location along the length of the micromixer starting from the 1st side jet. These images are joined together using the MATLAB code provided in Appendix C. The efficiency of the mixer for different flow ratios were calculated using the code at the beginning, end and average over the entire frames of the image set. The experimental

efficiency value at the exit of the mixer is referenced using the simulation value at the same location and values at other locations are evaluated corresponding to this referenced value. The combined plots of the simulation results for different flow ratios and corresponding referenced experimental efficiencies are given below. The combined micromixer image under room lights and also combined images from Rhodamine B mixing experiments for different flow ratios is also shown.

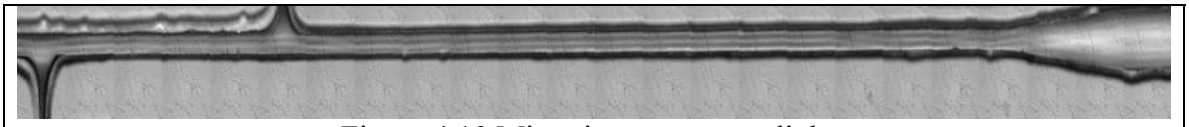

Figure 4.10 Mixer image at room lights

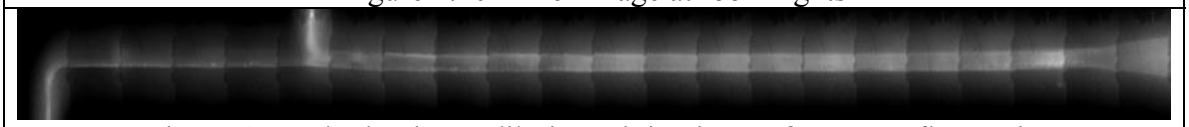

Figure 4.11 Rhodomine B dilution mixing image for 2.18:1 flow ratio

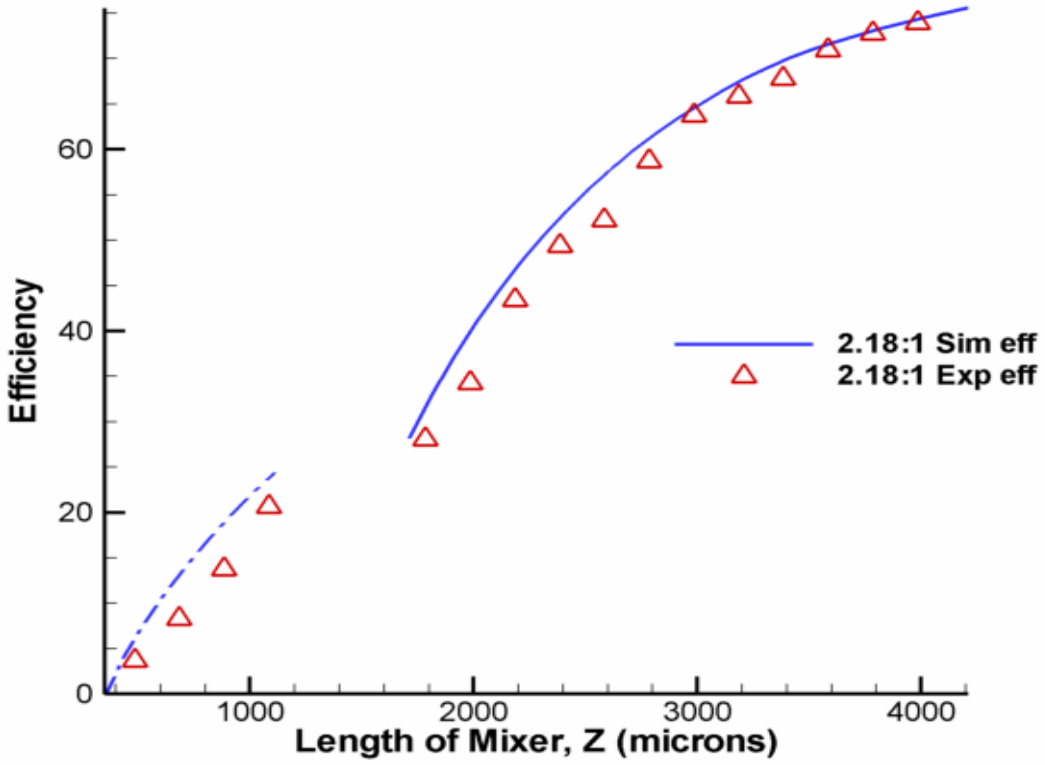

Figure 4.12 Comparing simulation and experimental efficiencies of jets in cross flow mixer with 1mm offset at 2.18:1 flow ratio

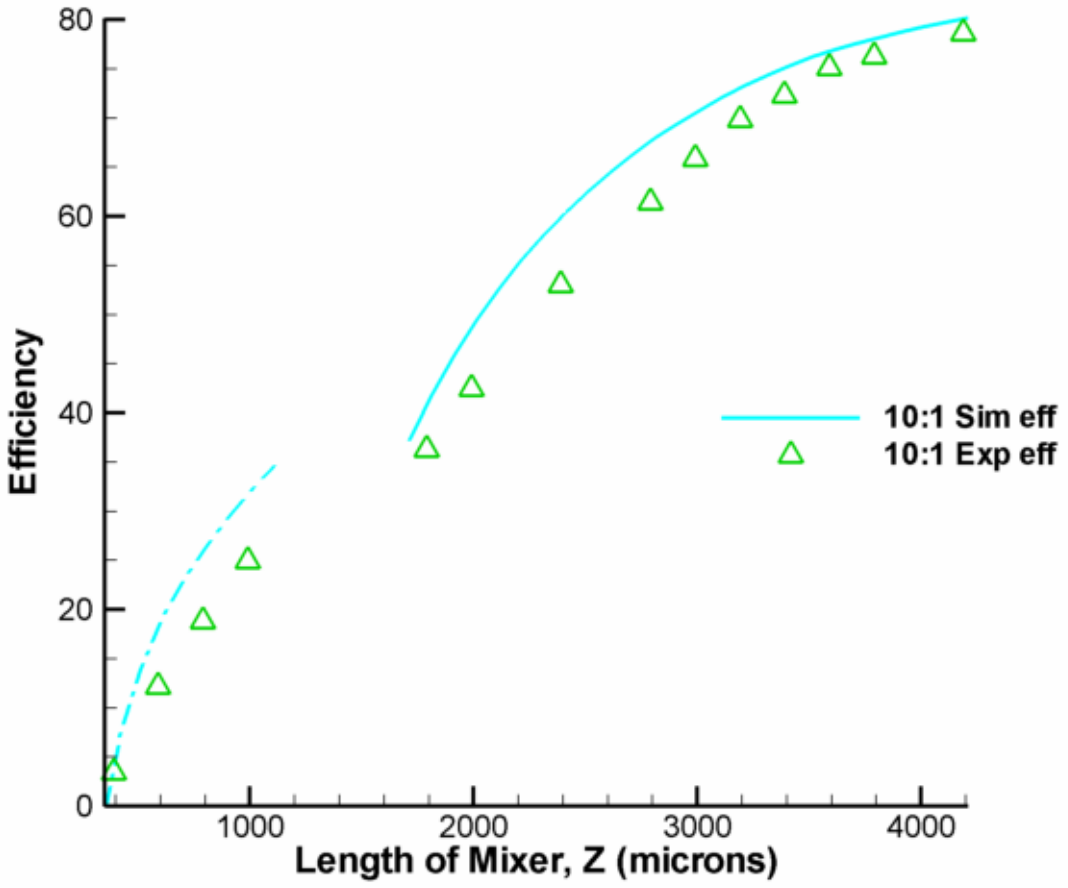

Figure 4.13 Comparing simulation and experimental efficiencies of jets in cross flow mixer with 1mm offset at 10:1 flow ratio

As explained earlier, the efficiency for ten to one flow ratio in a jets in cross flow with an offset between jets is found to be higher than two to one flow ratio which can be accounted due to the three dimensional effects at the junction between the side jet and the main mixing channel.

The efficiencies are calculated for each image set along the length of the mixer to eliminate the bright spots on the images which might have occurred due to saturated pixels at that particular location.

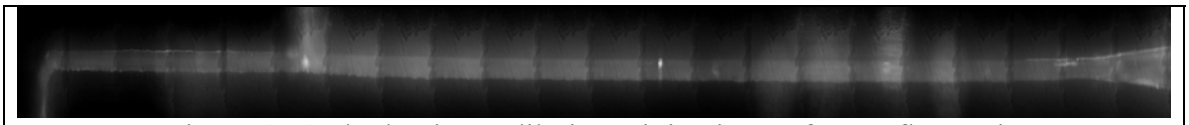

Figure 4.14 Rhodomine B dilution mixing image for 1:1 flow ratio

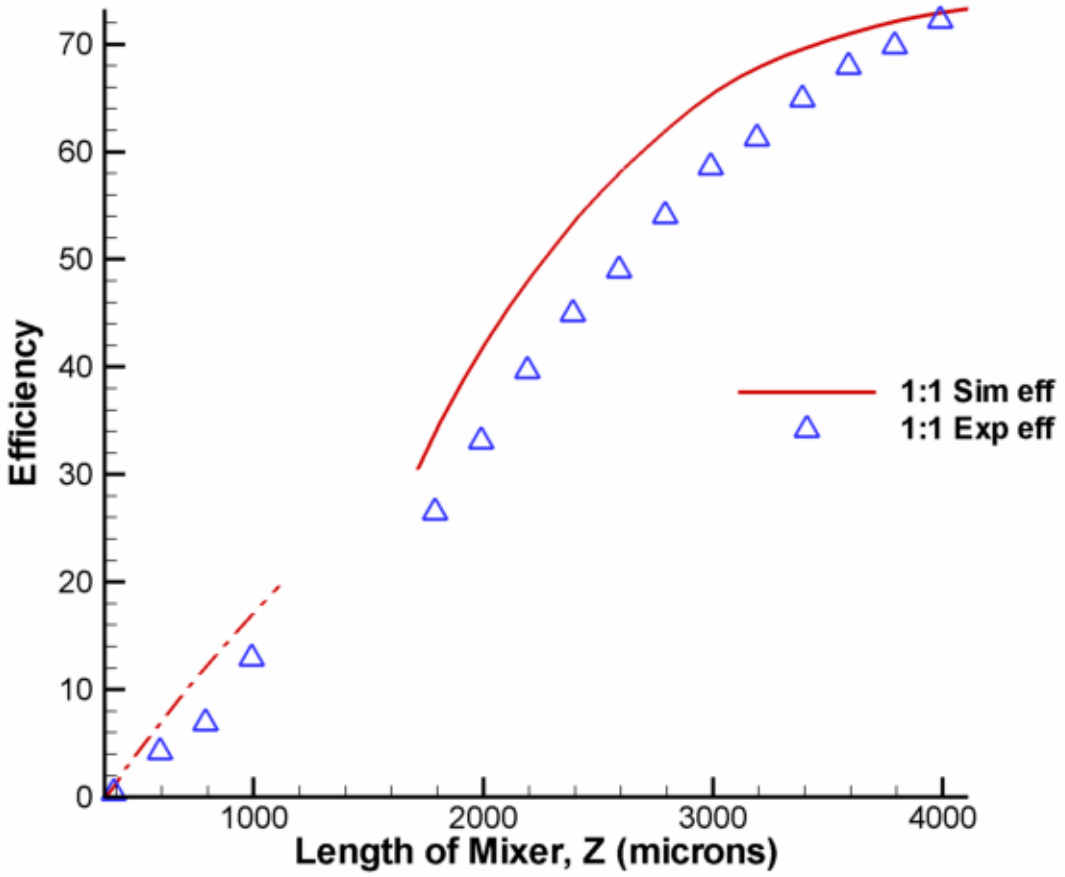

Figure 4.15 Comparing simulation and experimental efficiencies of jets in cross flow mixer with 1mm offset at 1:1 flow ratio

The bright spots in the mixing region for the images of ten to one and one to ten flow ratios are due to the saturated pixels at these particular locations. The average intensities for these flow ratios are therefore calculated by taking small window locations on the image sets not including the bright spots.

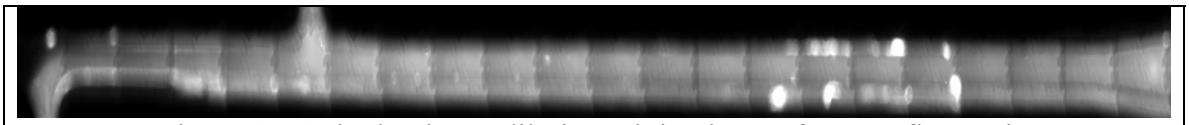

Figure 4.16 Rhodomine B dilution mixing image for 1:10 flow ratio

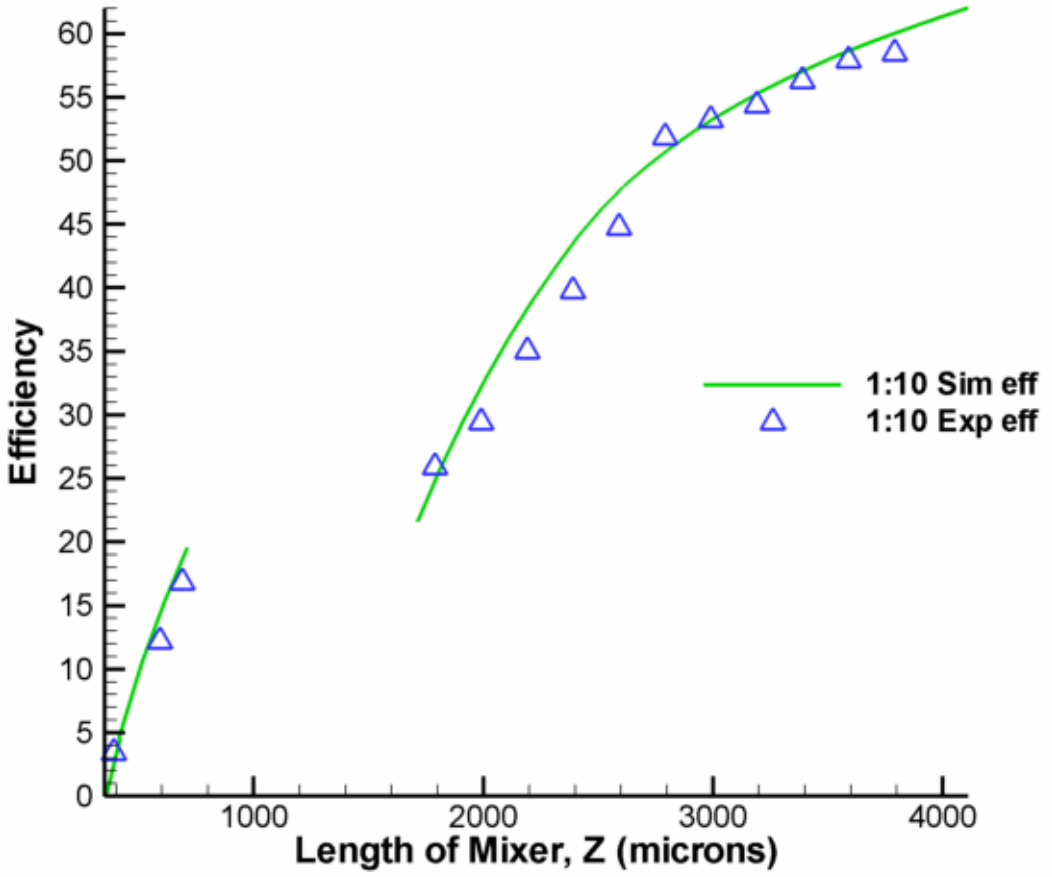

Figure 4.17 Comparing simulation and experimental efficiencies of jets in cross flow mixer with 1mm offset at 1:10 flow ratio

For one to ten flow ratio, the amount of Rhodomine dye entering from the side jets is much large when compared to the water which is entering through the main channel. The fluorescence significance can be seen from the Figure 4.15, which is found to be high when compared to ten to one flow ratio from Figure 4.11

4.6.3 Pressure Drops

Pressures are calculated at the inlet and exit of the mixer for jets in cross flow

with no offset and jets in cross flow with jets placed at an offset for all the flow ratios and are tabulated in the Table 4.2.

Table 4.2 Pressure Drops

	Flow Ratio	Inlet Pressure (Pa)	Side Jet Inlet Pressure (Pa)	Exit Pressure (Pa)	Pressure Drop (Pa)
X2J no offset	1:1	-26.828	29.18	-208.177	237.4
	1:10	-25.75	28.55	-208.03	236.6
	10:1	-48.62	-86.64	-253.734	205.0
	2.18:1	-36.8	-24.11	-228.85	204.7

	Flow Ratio	Center Inlet Pressure (Pa)	Side Jet1 Inlet Pressure (Pa)	Side Jet2 Inlet Pressure (Pa)	Exit Pressure (Pa)	Max. Pressure Drop (Pa)
X2J 1mm offset	1:1	-13.88	-33.63	-254.34	-1149.73	1136
	1:10	-2.674	2.33	-157.0	-1052.18	1055
	10:1	-26.8	-85.73	-357.3	-1247.97	1221
	2.18:1	-20.205	-59.3	-294.82	-1194.82	1175

The pressure drop is the maximum difference between the inlet and exit pressure of the mixers. The pressure drops for different flow ratios of jets in cross flow mixer with no offset mixer fall in the same range. While in case of jets in cross flow with an offset mixer, the pressure drop for 1:10 flow ratio is low compared to the other flows. As discussed earlier, the 10:1 flow ratio has higher efficiency of mixing at the cost of higher pressure drop, while 2.18:1 flow ratio has efficiency less than 10:1 but higher than 1:1 and 1:10, and considerably low pressure drop compared to 10:1. The pressure drop across the mixer should be taken into account while selecting the mixer and the flow ratio that is to be used for mixing fluids.

4.7 Conclusions

Hot embossed experimental chips with micromixer designs onto PMMA substrates using micro-milled brass mold insert are produced. Simulations on jets in cross flow mixer designs (no offset and 1mm offset) are performed for different flow ratios. Rhodamine B fluorescence solution was used in experimentally evaluating mixing efficiency of jets in cross flow micromixer for different flow ratios. The experimental efficiencies show good comparison with the simulation values for different flow ratios. As explained, the higher efficiency in the case of ten to one flow may be due to the three dimensional effects that occur at the junction where the three jets meet in the mixing channel. Experiments using a confocal microscope would provide more details of this behavior in the mixing region.

For a required amount of mixed product at a given time, the ten to one flow ratio in jets in cross flow mixer would give better performance compared to other flow ratios, with an increase in pressure drop between inlet and exit port. Whereas a flow ratio of 2.18:1 can be used for considerable amount of mixing at low pressure drops. For faster mixing to produce specific amount of mixed product, the jets in cross flow mixer with no offset design can be used at higher pressure drops.

Chapter 5. Conclusions and Future Work

This work is focused on manufacturing and characterization of jets in cross flow micro mixers, an optimum mixer design evaluated based on mixing efficiency and pressure drop criteria for particular type of applications.

Theory predictions have shown that mixing fluids in a three stream micro mixer, with an aspect ratio of three and above, at a flow ratio of 2.2 would yield better mixing efficiency when the delivery of the mixed product at a short time is considered as the main criteria.

Micromilled brass mold insert with features having an aspect ratio of about 12 was manufactured. This mold insert was used to hot-emboss micro channels onto PMMA substrate. Inlet reservoirs are drilled into these channels, which are then thermally bonded with a PMMA cover sheet of 125μm. Metrology is performed on the mixer mold insert using stylus profilometer at different critical locations to measure the feature height on the mold insert. Scanning Electron Microscope images are taken at the same locations and widths of these channels are measured. Using Student-t distribution analysis, the tolerance limits at each of the manufacturing method are determined. Mixing experiments are performed on these channels to compare with the simulation results.

Metrology results show a variation of dimensions by 5% compared to the design dimensions. Micro mixers having an aspect ratio of twelve were manufactured and are used for experiments. These mixers are developed on PMMA substrate, a material compatible with bio-related lab-on-chip equipment. Experimental results show close agreement with numerical simulation estimates.

Future work has to be concentrated in developing the manufacturing techniques to produce much higher aspect ratio micro channels that enhance diffusive mixing. The design dimensions are to be laid out keeping in view the manufacturing tolerances determined through our current work. Further experiments involving line average based imaging techniques using confocal microscopy, to capture the fluorescence signature from the entire depth of the channel would provide greater accuracy in determining the efficiency of a mixer.

References

1. Nikitopoulos, D. E. and Maha A., Micromixers, in BioMEMS: Technologies and Applications, Wang, W-J and Soper A. Eds, Taylor and Francis, 2006

2. Evans J., Liepmann D., Pisano A.P., "Planar Laminar Mixer", IEEE 1997, 96-101

3. Hiroaki Suzuki., Chin-Ming Ho., "A MAGNETIC FORCE DRIVEN CHAOTIC MICRO-MIXER", IEEE 2002, 0-7803-7185-2, 40-43.

4. Lu L. H., Ryu K. S., Liu C., "A Magnetic Microstirrer and Array for Microfluidic Mixing," Journal of Microelectromechanical Systems, 11(5), October 2002, 462-469

5. Oddy M.H., Santiago J. G., and Mikkelsen J.C., "Electrokinetic Instability Micromixing" Journal of Analytical Chemistry. 2001, Vol. 73, No. 24, 5822-5832.

6. Stroock, A.D., Dertinger, S.K.W., Ajdari, A., Mezic, E., Stone, H.A., Whitesides, G.M., "Chaotic Mixer for Microchannels," Science 295, 2002, 647-651

7. Maha A, Barrett D.O., Nikitopoulos D.E., Soper S.A., Murphy M.C., "Simulation and Design of Micro-Mixers for Microfluidic Devices", in MicroFluidics, BioMEMS, and Medical Microsystems II, ed H. Becker and P. Wolas, Society of Photo-optical Instrumentation Engineers (SPIE), 2003.

8. Liu R.H., Stremler M.A., Sharp K.V., Olsen M.G., Santiago J.G., Adrian R.J., Aref H., and Beebe D.J., " Passive Mixing in a Three-Dimensional Serpentine Microchannel," Journal of Microelectromechanical Systems 9 (2), June 2000, 190-197

9. Chung Y.C., Hsu Y.L., Jen C.P., Lu M.C., Lin Y.C., "Design of Passive Mixers Utilizing Microfluidic Self-circulation in the Mixing Chamber", Lab Chip, 4(1), 2004, 70-7.

10. Barrett, D.O., "Design of a Microfabricated device for Ligase Detection Reaction (LDR)", Master's Thesis, Louisiana State University, Baton Rouge, LA, 2004.

11. Bejat Y.D., "Micro-Chip Design, Numerical Simulation and Micro-PIV Diagnostics for DNA Assays", Master's Thesis, Louisiana State University, Baton Rouge, LA, 2001.

12. Meinhart C.D., Wereley S.T., Santiago J.G., "PIV measurement of a microchannel flow. Experiments in Fluids 27, 1999, 414 - 419.

Appendix A: Fortran Files to Calculate Mixing Efficiency

A.1 Calculate the Efficiency Based on Different Definitons for Varying Flow ratios: code by Dimitris E. Nikitopoulos

```
      parameter( nvars=7, npts_x=26, npts_y=151)
      dimension daray(nvars,2*npts_x*npts_y)
                dimension x(npts_x), y(npts_y), vars(nvars-2,npts_x,npts_y)
                dimension Dx(npts_x), Dy(npts_y), DA(npts_x,npts_y)
      character*55 datafileIN,datafileOUT
                npts=npts_x*npts_y
                open(10,file='IOList_1_1.txt',status='old')
                open(11,file='Eff_1_1.txt',status='unknown')
                read(10,*) numfiles
                do 1000 kk=1,numfiles
                        daray(1:nvars,1:npts)=0.0
                        vars(1:(nvars-2),1:npts_x,1:npts_y)=0.0
                        x(1:npts_x)=0.0
                        y(1:npts_y)=0.0
                        Dx(1:npts_x)=0.0
                        Dy(1:npts_y)=0.0
                        DA(1:npts_x,1:npts_y)=0.0
                        read (10,*) datafileIN
                        read (10,*) datafileOUT
                        read (10,*) z_plane
                        read (10,*) florat
                        read (10,*) mdualzone
                        write (*,*) datafileIN
                        write (*,*) datafileOUT
                        write (*,*) z_plane
                        write (*,*) florat
                        write (*,*) mdualzone
! provide input data file
!               datafile='X2J_no_offset_v1_1_1_flow_z_214.txt'
! Set Flow ratio
!               florat=1.
! If there is a dual zone from channel extension combination set to 1
! otherwise set to 0
!               mdualzone=0
                npts=npts_x*npts_y
                if (mdualzone==1) npts=2*npts
                open(9,file=datafileIN,status='old')
                do 10 j=1,npts
                        read(9,*) (daray(i,j),i=1,nvars)
```

```
!                       if (daray(2,j)==0) then
!                       daray(4:(nvars-1),j)=0.0
!                       endif
!                       if (daray(1,j)==12.5) then
!                       daray(4:(nvars-1),j)=0.0
!                       endif
!                       write(*,*) (daray(i,j),i=1,nvars)
!                       pause
10              continue
                if (mdualzone==1) then
                        do 20 j=1,npts/2
                                daray(1:nvars,j)=(daray(1:nvars,(2*j-
1))+daray(1:nvars,(2*j)))/2
20                      continue
                endif
                do 14 k=4,6
                        do 24 j=1,npts_y
                                daray(k,((npts_x-1)*npts_y+j))=0.0
                                do 34 i=1,npts_x
                                        daray(k,((i-1)*npts_y+1))=0.0
34                              continue
24                      continue
14              continue
                do 15 i=1,npts_x
                        x(i)=daray(1,((i-1)*npts_y+1))
                        do 25 j=1,npts_y
                                y(j)=daray(2,j)
                                do 35 k=3,nvars
                                        vars(k-2,i,j)=daray(k,((i-1)*npts_y+j))
35                              continue
25                      continue
15              continue
!               do 40 k=2,4
!                       vars(k,npts_x,1:npts_y)=0.0
!                       vars(k,1:npts_x,1)=0.0
!40             continue
                close(9,status='keep')
                do 36 i=2,npts_x-1
                        Dx(i)=(x(i+1)-x(i-1))/2
36              continue
                do 26 j=2,npts_y-1
                        Dy(j)=(y(j+1)-y(j-1))/2
26              continue
                        Dx(1)=(x(2)-x(1))/2
                        Dx(npts_x)=(x(npts_x)-x(npts_x-1))/2
                        Dy(1)=(y(2)-y(1))/2
```

```
                Dy(npts_y)=(y(npts_y)-y(npts_y-1))/2
        Atot=0.0
        cAtot=0.0
        cinf=0.0
        Qtot=0.0
        do 37 i=1,npts_x
                do 27 j=1,npts_y
                        DA(i,j)=Dx(i)*Dy(j)
                        cDA=vars(5,i,j)*DA(i,j)
                        QDA=vars(4,i,j)*DA(i,j)
                        cinfDA=vars(5,i,j)*vars(4,i,j)*DA(i,j)
                        Atot=Atot+DA(i,j)
                        cAtot=cAtot+cDA
                        Qtot=Qtot+QDA
                        cinf=cinf+cinfDA
27              continue
37      continue
        cAtot=cAtot/Atot
        Um=Qtot/Atot
        cinf=cinf/Qtot
        Qtot=Qtot/1000.0
        RMSccinf=0.0
        RMSccA=0.0
        AcApos=0.0
        Acinfpos=0.0
        AcAneg=0.0
        Acinfneg=0.0
        RMSccinfpos=0.0
        RMSccApos=0.0
        RMSccinfneg=0.0
        RMSccAneg=0.0
!
                ABSccinfpos=0.0
                ABSccinfneg=0.0
                ABSccApos=0.0
                ABSccAneg=0.0
        RMSQccinf=0.0
        ABSccinf=0.0
        ABSccA=0.0
        ABSQccinf=0.0
        do 38 i=1,npts_x
                do 28 j=1,npts_y
                        RMSccADA=(vars(5,i,j)-cAtot)*(vars(5,i,j)-cAtot)*DA(i,j)
                        RMSccinfDA=(vars(5,i,j)-cinf)*(vars(5,i,j)-cinf)*DA(i,j)
!
                        RMSQccinfDA=RMSccinfDA*vars(4,i,j)*vars(4,i,j)
```

```
                        ABSccADA=abs(vars(5,i,j)-cAtot)*DA(i,j)
                        ABSccinfDA=abs(vars(5,i,j)-cinf)*DA(i,j)
                        ABSQccinfDA=abs(vars(5,i,j)-cinf)*vars(4,i,j)*DA(i,j)
!
                        RMSccA=RMSccA+RMSccADA
                        RMSccinf=RMSccinf+RMSccinfDA
!
                        RMSQccinf=RMSQccinf+RMSQccinfDA
                        ABSQccinf=ABSQccinf+ABSQccinfDA
                        ABSccA=ABSccA+ABSccADA
                        ABSccinf=ABSccinf+ABSccinfDA
                        if ((vars(5,i,j)-cinf)>=0) then
                                Acinfpos=Acinfpos+DA(i,j)
                                RMSccinfpos=RMSccinfpos+RMSccinfDA
                           ABSccinfpos=ABSccinfpos+ABSccinfDA
                        else
                                Acinfneg=Acinfneg+DA(i,j)
                                RMSccinfneg=RMSccinfneg+RMSccinfDA
                           ABSccinfneg=ABSccinfneg+ABSccinfDA
                        endif
                        if ((vars(5,i,j)-cAtot)>=0) then
                                AcApos=AcApos+DA(i,j)
                                RMSccApos=RMSccApos+RMSccADA
                                ABSccApos=ABSccApos+ABSccADA
                        else
                                AcAneg=AcAneg+DA(i,j)
                                RMSccAneg=RMSccAneg+RMSccADA
                                ABSccAneg=ABSccAneg+ABSccADA
                        endif
28                  continue
38              continue
                RMSccinf=sqrt(RMSccinf/Atot)
                RMSccA=sqrt(RMSccA/Atot)
                RMSccinfpos=sqrt(RMSccinfpos/Acinfpos)
                RMSccApos=sqrt(RMSccApos/AcApos)
                RMSccinfneg=sqrt(RMSccinfneg/Acinfneg)
                RMSccAneg=sqrt(RMSccAneg/AcAneg)
!
                        ABSccinfpos=(ABSccinfpos/Acinfpos)
                        ABSccApos=(ABSccApos/AcApos)
                        ABSccinfneg=(ABSccinfneg/Acinfneg)
                        ABSccAneg=(ABSccAneg/AcAneg)
                RMSQccinf=sqrt(RMSQccinf/Atot)
                ABSccinf=(ABSccinf/Atot)
                ABSccA=(ABSccA/Atot)
                ABSQccinf=(ABSQccinf/Atot)
```

```
!
      open(8,FORM='FORMATTED',access='SEQUENTIAL',file='sink',status='unkno
wn')
!               do 30 j=1,npts/2
!                     write(8,'(7E12.5)') (daray(i,j),i=1,nvars)
!30             continue
!               close(8,status='keep')
!               datafile='X2J_no_offset_v1_10_1_flow_Ext_joined_Z_1300_outv2'

      open(7,FORM='FORMATTED',access='SEQUENTIAL',file=datafileOUT,status
='unknown')
!               do 45 i=1,npts_x
!                     do 50 j=1,npts_y
!                           write (7,'(7E12.5)') x(i),y(j),(vars(k,i,j),k=1,nvars-2)
!50                   continue
!45             continue
!               do 46 i=1,npts_x
!                     do 51 j=1,npts_y
!                           write (7,'(7E12.5)') x(i), y(j), Dx(i), Dy(j), DA(i,j)
!51                   continue
!46             continue
                     write (7,*) datafileIN
                     write (7,*) datafileOUT
                     write (7,*) z_plane
                     write (7,*) florat
                     write (7,*) mdualzone
               write (7,'(3(A5,E12.5,A5))') '   A=',Atot,' um^3','   Q=',Qtot,' nL/s','
Um=',Um,' mm/s'
               write (*,'(3(A5,E12.5,A5))') '   A=',Atot,' um^3','   Q=',Qtot,' nL/s','
Um=',Um,' mm/s'
               write (7,'(2(A15,E12.5))') '        cinf=',cinf,      '         cav=',cAtot
               write (*,'(2(A15,E12.5))') '        cinf=',cinf,      '         cav=',cAtot
               write (7,'(2(A15,E12.5))') '    cRMScinf=',RMSccinf,  '
cRMSccA=',RMSccA
               write (*,'(2(A15,E12.5))') '    cRMScinf=',RMSccinf,  '
cRMSccA=',RMSccA
               write (7,'(2(A15,E12.5))') '    cABScinf=',ABSccinf,  '
cABSccA=',ABSccA
               write (*,'(2(A15,E12.5))') '    cABScinf=',ABSccinf,  '
cABSccA=',ABSccA
               write (7,'(2(A15,E12.5))') '   cRMSQcinf=',RMSQccinf, '         nL/s'
               write (*,'(2(A15,E12.5))') '   cRMSQcinf=',RMSQccinf, '         nL/s'
               write (7,'(2(A15,E12.5))') '   cABSQcinf=',ABSQccinf, '         nL/s'
               write (*,'(2(A15,E12.5))') '   cABSQcinf=',ABSQccinf, '         nL/s'
               RMSccinf=RMSccinf/cinf*100.
               RMSccA=RMSccA/cAtot*100.
```

```
                RMSccinfpos=RMSccinfpos/cinf*100
                RMSccApos=RMSccApos/cAtot*100
                RMSccinfneg=RMSccinfneg/cinf*100
                RMSccAneg=RMSccAneg/cAtot*100
                        ABSccinfpos=ABSccinfpos/cinf*100
                        ABSccApos=ABSccApos/cAtot*100
                        ABSccinfneg=ABSccinfneg/cinf*100
                        ABSccAneg=ABSccAneg/cAtot*100
                efcinfpos=(1-RMSccinfpos/(florat*100))*100
                efcinfneg=(1-RMSccinfneg/(100))*100
                efcinf=efcinfpos*Acinfpos/Atot+efcinfneg*Acinfneg/Atot
                efcinfABSpos=(1-ABSccinfpos/(florat*100))*100
                efcinfABSneg=(1-ABSccinfneg/(100))*100
                efcinfABS=efcinfABSpos*Acinfpos/Atot+efcinfABSneg*Acinfneg/Atot
                write (7,'(2(A15,F7.2))') '     cRMS%cinf=',RMSccinf,   '
cRMS%ccA=',RMSccA
                write (*,'(2(A15,F7.2))') '     cRMS%cinf=',RMSccinf,   '
cRMS%ccA=',RMSccA
                write (7,'(2(A15,F7.2))') '       AcApos=',AcApos,     '
AcAneg=',AcAneg
                write (*,'(2(A15,F7.2))') '       AcApos=',AcApos,     '
AcAneg=',AcAneg
                write (7,'(2(A15,F7.2))') '   cRMS%ccApos=',RMSccApos,  '
cRMS%ccAneg=',RMSccAneg
                write (*,'(2(A15,F7.2))') '   cRMS%ccApos=',RMSccApos,  '
cRMS%ccAneg=',RMSccAneg
                write (7,'(2(A15,F7.2))') '      Acinfpos=',Acinfpos,   '
Acinfneg=',Acinfneg
                write (*,'(2(A15,F7.2))') '      Acinfpos=',Acinfpos,   '
Acinfneg=',Acinfneg
                write (7,'(2(A15,F7.2))') ' cRMS%ccinfpos=',RMSccinfpos,'
cRMS%ccinfneg=',RMSccinfneg
                write (*,'(2(A15,F7.2))') ' cRMS%ccinfpos=',RMSccinfpos,'
cRMS%ccinfneg=',RMSccinfneg
                write (7,'(2(A15,F7.2))') ' cABS%ccinfpos=',ABSccinfpos,'
cABS%ccinfneg=',ABSccinfneg
                write (*,'(2(A15,F7.2))') ' cABS%ccinfpos=',ABSccinfpos,'
cABS%ccinfneg=',ABSccinfneg
                write (7,'(3(A15,F7.2))') '     efcinfpos=',efcinfpos,  '
efcinfneg=',efcinfneg,'       efcinf=',efcinf
                write (*,'(3(A15,F7.2))') '     efcinfpos=',efcinfpos,  '
efcinfneg=',efcinfneg,'       efcinf=',efcinf
                write (7,'(3(A15,F7.2))') '  efcinfABSpos=',efcinfABSpos,'
efcinfABSneg=',efcinfABSneg,'     efcinfABS=',efcinfABS
                write (*,'(3(A15,F7.2))') '  efcinfABSpos=',efcinfABSpos,'
efcinfABSneg=',efcinfABSneg,'     efcinfABS=',efcinfABS
```

```
                if (kk==1) then
                Atot0=Atot
                Qtot0=Qtot
                Um0=Um
                cinf0=cinf
                cAtot0=cAtot
                RMSccinf0=RMSccinf
                RMSccA0=RMSccA
                ABSccinf0=ABSccinf
                ABSccA0=ABSccA
                RMSQccinf0=RMSQccinf
                ABSQccinf0=ABSQccinf
                RMSccinf0=RMSccinf
                RMSccA0=RMSccA
                AcApos0=AcApos
                AcAneg0=AcAneg
                RMSccApos0=RMSccApos
                RMSccAneg0=RMSccAneg
                Acinfpos0=Acinfpos
                Acinfneg0=Acinfneg
                RMSccinfpos0=RMSccinfpos
                RMSccinfneg0=RMSccinfneg
                efcinfpos0=efcinfpos
                efcinfneg0=efcinfneg
                efcinf0=efcinf
                efcinfABSpos0=efcinfABSpos
                efcinfABSneg0=efcinfABSneg
                efcinfABS0=efcinfABS
                endif
                efRMSQcinf=(1-RMSQccinf/RMSQccinf0)*100.
                efABSQcinf=(1-ABSQccinf/ABSQccinf0)*100.
                efABSccinf=(1-ABSccinf/ABSccinf0)*100.
                efABScA=(1-ABSccA/ABSccA0)*100.
                write (11,'(12F8.2)')
florat,z_plane,efcinfpos,efcinfneg,efcinf,efcinfABSpos,efcinfABSneg,efcinfABS,efRMS
Qcinf,efABSQcinf,efABSccinf,efABScA
                write (7,'(2(A15,F7.2))') '    efRMSQcinf=',efRMSQcinf, '
efABSQcinf=',efABSQcinf
                write (*,'(2(A15,F7.2))') '    efRMSQcinf=',efRMSQcinf, '
efABSQcinf=',efABSQcinf
                write (7,'(2(A15,F7.2))') '     efABSccinf=',efABSccinf,  '
efABScA=',efABScA
                write (*,'(2(A15,F7.2))') '     efABSccinf=',efABSccinf,  '
efABScA=',efABScA
```

```
                write (*,*)
'*****************************************************************************
******'
                close(7,status='keep')
1000    continue
                close(10,status='keep')
                close(11,status='keep')
                write (*,'(3(A5,E12.5,A5))') '   A=',Atot0,' um^3','   Q=',Qtot0,' nL/s','
Um=',Um0,' mm/s'
                write (*,'(2(A15,E12.5))') '         cinf=',cinf0,      '          cav=',cAtot0
                write (*,'(2(A15,E12.5))') '     cRMScinf=',RMSccinf0,   '
cRMSccA=',RMSccA0
                write (*,'(2(A15,E12.5))') '     cABScinf=',ABSccinf0,   '
cABSccA=',ABSccA0
                write (*,'(2(A15,E12.5))') '    cRMSQcinf=',RMSQccinf0,  '          nL/s'
                write (*,'(2(A15,E12.5))') '    cABSQcinf=',ABSQccinf0,  '          nL/s'
                write (*,'(2(A15,F7.2))') '    cRMS%cinf=',RMSccinf0,   '
cRMS%ccA=',RMSccA0
                write (*,'(2(A15,F7.2))') '       AcApos=',AcApos0,     '
AcAneg=',AcAneg0
                write (*,'(2(A15,F7.2))') '  cRMS%ccApos=',RMSccApos0,  '
cRMS%ccAneg=',RMSccAneg0
                write (*,'(2(A15,F7.2))') '     Acinfpos=',Acinfpos0,   '
Acinfneg=',Acinfneg0
                write (*,'(2(A15,F7.2))') ' cRMS%ccinfpos=',RMSccinfpos0,'
cRMS%ccinfneg=',RMSccinfneg0
                write (*,'(3(A15,F7.2))') '    efcinfpos=',efcinfpos0,  '
efcinfneg=',efcinfneg0,'       efcinf=',efcinf0
                write (*,'(3(A15,F7.2))') '  efcinfABSpos=',efcinfABSpos0,'
efcinfABSneg=',efcinfABSneg0,'    efcinfABS=',efcinfABS0
                end
```

Appendix B: Matlab Files

B.1 Matlab File Used to Sort Tecplot Slice Data to run Appendix A FORTRAN Code

```
%%%%%%%%%%%%%%%%%%%%%%%%%%%%%%%%%%%%%%%%%%%%%%
%%%%%%
%Vamsi Palaparthy
%Program to sort data of a tecplot slice to run the FORTRAN code in
%Appendix A to calculate efficiency%%%%%%%
%%%%%%%%%%%%%%%%%%%%%%%%%%%%%%%%%%%%%%%%%%%%%%
%%%%%%

clear all;
clc;

data=load('C:\Documents and Settings\vamsi\Desktop\vamsi
simulations\X2J_no_offset_v1\DEN_Eff_code\z_slices_IOList_DEN_code\10_1\X2J_no
_offset_v1_10_1_flow_z_3112_5.txt');
x=[0:.5:12.5]'; %Range of x corresponding to the x nodal values in tecplot Z slice
y=[0:.5:75]';   %Range of y corresponding to the y nodal values in tecplot Z slice
z=1;            %Counter

for i=1:length(x) %Go from 1 upto the length of x values (=25)

        for k=1:length(y) %Go from 1 upto the length of y values (=150)

                for j=1:length(data(:,1)) %Go from 1 upto the length of 1st column in data
(all x %values = %25*150)

                if (data(j,1)==x(i,1)&data(j,2)==y(k,1)) % Compare the values of x and y
%in data and write entire %row in temp if they are equal

                        temp(z,:)=data(j,:);
                        z=z+1;   %increase the counter
                        end
        end

end

end

dlmwrite('C:\Documents and Settings\vamsi\Desktop\vamsi
simulations\X2J_no_offset_v1\DEN_Eff_code\z_slices_IOList_DEN_code\10_1\10_1_s
```

```
orted_data\X2J_no_offset_v1_10_1_flow_z_3112_5.txt', temp, 'delimiter', '\t', 'precision',
12);%write the %sorted data file in text format
%xlswrite('C:\Documents and Settings\vamsi\Desktop\vamsi
%simulations\X2J_no_offset_v1\DEN_Eff_code\z_slices_IOList_DEN_code\1_1\1_1_s
orted_data%\X2J_no_offset_v1_1_1_flow_z_412_5.xls',temp)
```

B2. Matlab File to Combine Images Ref: LSU Thesis Maha 2005

```
%%%%%%%%%%%%%%%%%%%%%%%%%%%%%%%%%%%%%%%%%%%%%%%%%%%%%%%%%%%%%%%%%%%%%%%%%%%%
% Vamsi Palaparthy
% Program to read images from a multi-image TIFF file
% Program combines the tiff images into a single file
%%%%%%%%%%%%%%%%%%%%%%%%%%%%%%%%%%%%%%%%%%%%%%%%%%%%%%%%%%%%%%%%%%%%%%%%%%%%

clc;                                        % Clear screen
clear all;                                  % Clear all variables from the memory


image_file_ext = '.tif';                    % Extension of the image file
num_image_sets = 22;                        % Number of image sets
m_pixel = 0.66;                             % microns per pixel
image_mismatch = 2;                         % Image mismatch in microns
delta_pixel = floor(200/m_pixel);
filepath = 'I:\Vamsi\Image_Processing\X2J_R50_Rhb_case4_opt_exp3\';
for n_images = 1 : num_image_sets
   image_filename = 'Image';                % Name of the multi-image TIFF file
assigned to image_filename variable
   image_filename = strcat(filepath, image_filename, num2str(n_images),
image_file_ext)      % Filename to read images based on the set or part
   imgfile_info = imfinfo(image_filename,'tif')          % Obtaining information
about the image_file variable
   [Img_X, map] = imread(image_filename, 1);     % read the first frame to
estimate the size of the image
   frame_size = size(Img_X);                    % Size of each frame
   no_of_columns = frame_size(2);               % Total number of Columns
per frame
   no_of_rows = frame_size(1);
   for i = 1 : delta_pixel
      for j = 1 : no_of_rows
         row_index = j+(n_images-1)*image_mismatch;     % Calculate row index
offset due to image sets misallignment
         if ( row_index > no_of_rows)
            Img_Y(j, floor((n_images-1)*delta_pixel) + i) = Img_X(j,i);
```

```
        else
           Img_Y(j, floor((n_images-1)*delta_pixel) + i) = Img_X(row_index,i);
        end
      end
   end
end
imwrite(Img_Y, map,
'I:\Vamsi\Image_Processing\X2J_R50_Rhb_case4_opt_exp3\X2J_R50_Rhb_case4_opt_
exp3_combined_image_v1.tif', 'Compression', 'none', 'Description', 'Combined Image',
'Resolution', [33 26], 'WriteMode', 'overwrite');
```

B3. Matlab File Used to Plot Calibration Curve Ref: LSU Thesis Maha 2005

```
%%%%%%%%%%%%%%%%%%%%%%%%%%%%%%%%%%%%%%%%%%%%%%%%%%%%%%%%%%%%%%%%
% Vamsi Palaparthy
% Program to read images from a multi-image TIFF file
%%%%%%%%%%%%%%%%%%%%%%%%%%%%%%%%%%%%%%%%%%%%%%%%%%%%%%%%%%%%%%%%

clc;                                        % Clear screen
clear all;                                  % Clear all variables from the memory

frame_index = 1;                            % Index number for the frame number
to read from the multi-image TIFF file
image_file_ext = '.tif';                    % Extension of the image file
num_image_sets = 10;                        % Number of image sets
num_frames =  80;                           % Number of frames
tecplot_datafile =
strcat('I:\Vamsi\Image_Processing\Rhb_case5_Calibration_Exp2\75um_from_surface\2n
d_jet\','Rhb_calib_case5_Curve_v1', '_tec.dat')
                                            % Create tecplot filename based on image
filename

fileptr = fopen(tecplot_datafile, 'w');     % open the tecplot data file for
appending
fprintf(fileptr, 'TITLE = "Rhb Calibration Curve"\nVARIABLES =
\n"Dilution"\n"Average Intensity"\n"Standard Deviation"\n"Concentration"\n');
fprintf(fileptr, 'ZONE T="Rhb Calibration Curve" \nI=10, F=POINT, DT=(DOUBLE,
DOUBLE, DOUBLE, DOUBLE)\n')

for n_images = 1 : num_image_sets
   image_filename = 'Rhb_calib_case5_';     % Name of the multi-image
TIFF file assigned to image_filename variable
   file_nmbr = n_images*10;                 % File number generated based on
loop counter
```

```
   image_filename = strcat(image_filename,num2str(file_nmbr), image_file_ext)      % Filename to read images based on the set or part

   min_row_ind = 120;                          % Min index for row to calculate average
   max_row_ind = 140;                          % Max index for row to calculate average
   min_col_ind = 180;                          % Min index for column to calculate average
   max_col_ind = 200;                          % Max index for column to calculate average
   Int_array = zeros(1);                       % Initialize the Intensity array

      for frame_index = 1 : num_frames                          % Loop to go over all the frames
         frame_index                                            % Display frame index number
         [Img_X, map] = imread(image_filename, frame_index);    % read the frame # based on index used
         count = 1;                                             % Counter for the Intensity Array

         for j = min_col_ind : max_col_ind                      % Loop to go over the columns
            for i = min_row_ind : max_row_ind                   % Loop to go over the rows
               temp_sub = double(Img_X(i,j)) + 1;               % 1 index offset as matlab index starts from 1
               Int_array(count,1) = map(temp_sub, 1);           % Intensity Array to calculate mean, std etc

               count = count + 1;                               % Increment the counter
            end                                                 % End for the column loop
         end                                                    % End for the row loop

      end                                                       % End for the frame loop
      Dilution = file_nmbr;
      mean_intensity = mean(Int_array)                          % Calculate the mean intensity from the array
      std_intensity = std(Int_array)                            % Calculate the standard intensity for intensity from the array
      Concentration = Dilution*1.44e-6/100;                     % Calculate the concentration for each dilution

      fprintf(fileptr, '%15.9f %15.9f %15.9f %15.9f\n', Dilution, mean_intensity, std_intensity, Concentration);
      % Write to the tecplot data file

end
status = fclose(fileptr);                                       % Close the tecplot data file
```

Appendix C: AutoCAD Micromixer Drawings

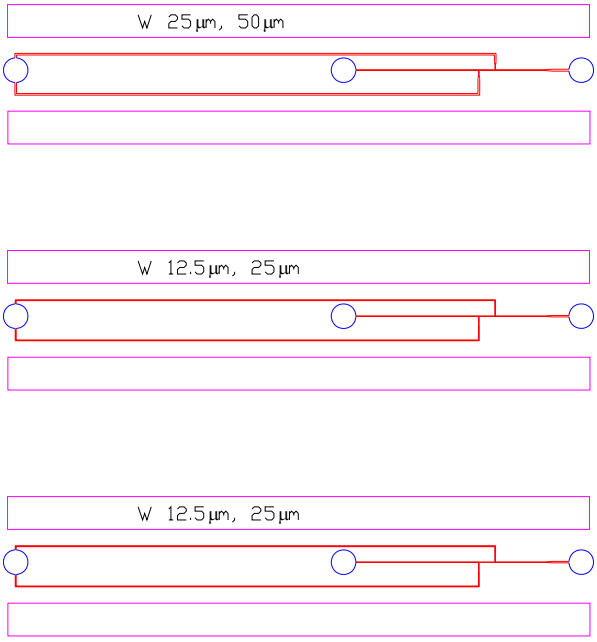

Figure C.1: AutoCAD drawing layout for X2J mixers manufactured by micromilling

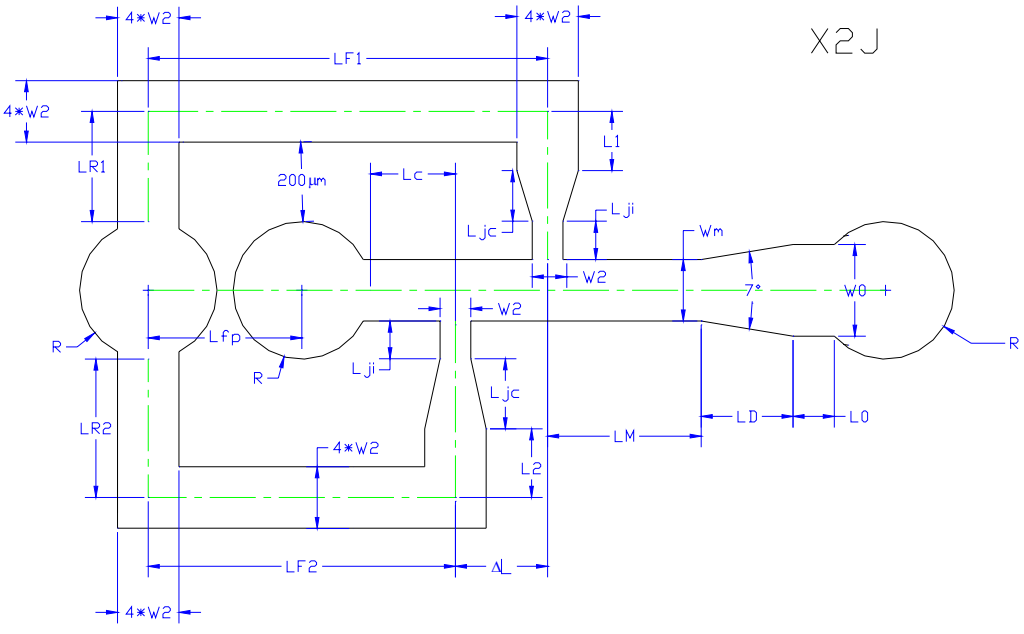

Figure C.2: X2J micromixer drawing layout details

Vita

Vamsi Palaparthy was born in Hyderabad, Andhra Pradesh, India, in 1981. He completed his high school studies in 1999. He received his Bachelor of Engineering in Industrial/Production Engineering from Vasavi College of Engineering, affiliated to the Osmania University in June 2003. He joined the graduate program at Louisiana State University in Fall 2003. He expects to receive his master's degree in May 2007.